Accepted Manuscript

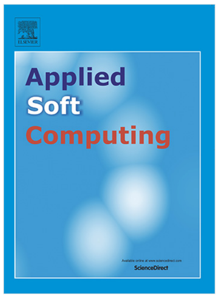

Structural damage detection using imperialist competitive algorithm and damage function

Saleheh Gerist, Mahmoud R. Maheri

PII: S1568-4946(18)30733-6
DOI: https://doi.org/10.1016/j.asoc.2018.12.032
Reference: ASOC 5265

To appear in: *Applied Soft Computing Journal*

Received date : 19 December 2017
Revised date : 3 October 2018
Accepted date : 27 December 2018

Structural Damage Detection using Imperialist Competitive Algorithm and Damage Function

Saleheh Gerist[a] and Mahmoud R Maheri[b]

[a] PhD candidate, Department of Civil Engineering, Shiraz University, Email: zgerist@gmail.com
[b] Professor of Civil Engineering, Shiraz University, Email: maheri@shirazu.ac.ir

Abstract

In practical damage detection problems, experimental modal data is only available for a limited number of modes and in each mode, only a limited number of nodal points are recorded. In using modal data, the majority of the available damage detection solution techniques either require data for all the modes, or all the nodal data for a number of modes; neither of which may be practically available through experiments. In the present study, damage identification is carried out using only a limited number of nodal data of a limited number of modes. The proposed method uses the imperialist competitive optimisation algorithm and damage functions. To decrease the number of design variables, several bilinear damage functions are defined to model the damage distribution. Damage functions with both variable widths and variable weights are proposed for increased accurately. Four different types of objective functions which use modal responses of damaged structure are investigated with the aim of finding the most suitable function. The efficiency of the proposed method is investigated using three benchmark numerical examples using both clean and noisy modal data. It is shown that by only using a limited number of modal data, the proposed method is capable of accurately detecting damage locations and reasonably accurately evaluate their extents. The proposed algorithm is most effective with noisy modal data, compared to other available solutions.

Keywords: *Damage detection; imperialist competitive method; damage function; modal data; noisy response; finite element method.*

Graphical abstract:

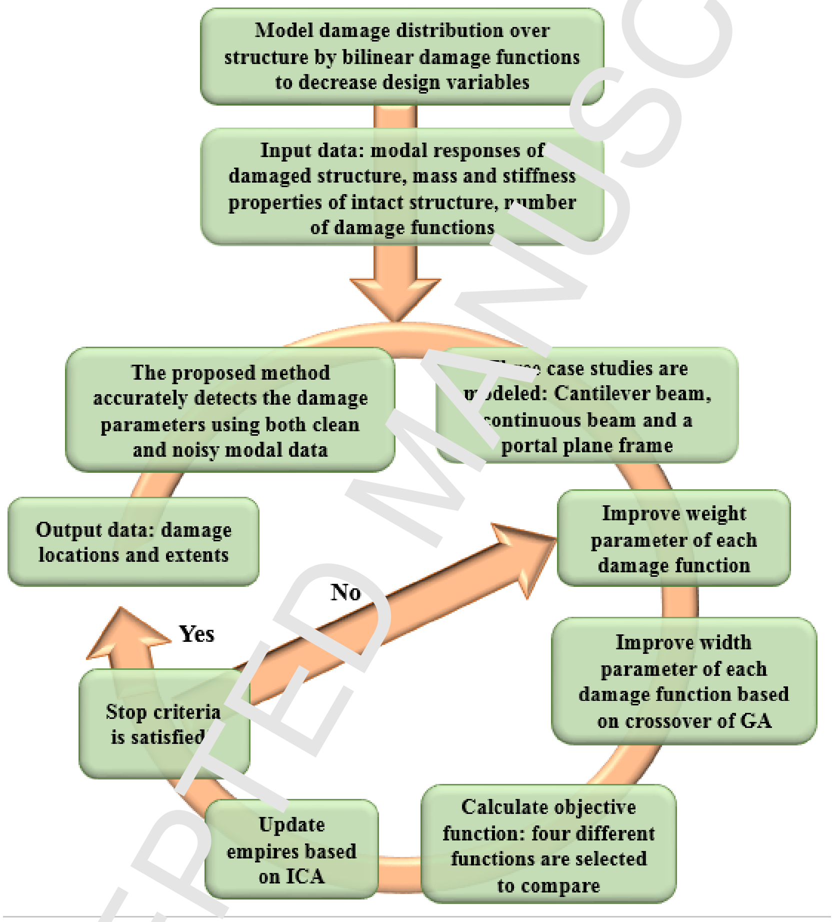

1. Introduction

Damage detection is one of the most active fields of research which has attracted a great deal of interest in recent years [1, 2]. Damage detection techniques have been successfully applied to many practical problems to identify damage through non-destructive tests (NDT). Damage causes a change in the physical properties of the structure, mainly its stiffness, resulting in changes in the dynamic properties of the system such as its natural frequencies, mode shapes, damping ratios and modal strain energies. Therefore, the location of damage and its extent could be identified by monitoring one or more of these properties of the damaged structure.

Optimization techniques have long been employed to solve different problems [3, 4], including damage detection problems [5]. Some recent examples may be found in references [6-8]. Genetic algorithm (GA) is a global optimization technique which has recently been improved and hybridized with other meta-heuristic methods to solve damage detection problems [9-11]. Particle swarm optimization (PSO) is also a useful optimization technique which is frequently applied in the area of topology and shape optimization of structures [12, 13]. PSO has also been used to solve damage detection problems [14, 15]. For a comprehensive review of hybridization of metaheuristic and mathematical programming methods, we refer the interested reader to the survey in [4] and the works [3] and [16]. A hybridization of PSO and linear programming was adopted recently to solve damage detection problems [17]. Another, powerful meta-heuristic algorithm is the imperialist competitive algorithm (ICA), proposed by Atashpaz-Gargari and Lucas to solve optimization problems [18]. This algorithm is a socio-politically motivated optimization algorithm and has shown great performance in both convergence rate and better identification of global optima. Its applicability, effectiveness and limitations were investigated in [19]. Researchers have applied the ICA to solve different optimization problems [19-22]. The ICA was compared with the GA and PSO algorithms by Dossary and Nasrabadi [20]. They concluded that the ICA converges to better solution in a fixed number of simulation runs. Maheri and Talezadeh [21] proposed an enhanced imperialist competitive algorithm (EICA). The algorithm was improved by giving added value to a slightly unfeasible solution, based on its distance from the relative imperialist. Their results showed that, EICA compares significantly favourable with a number of other meta-heuristic optimizers, including the basic ICA. Damage identification was formulated as an optimization problem and solved by the imperialist competitive algorithm in [22] and [23]. An error function using modal responses, stiffness and mass matrices were used to solve the problem in [22]. They used all the mode shapes data to calculate objective function of the algorithm and concluded that the method was much more sensitive to location and value of damage compared with the energy index method and converged to correct solution even in the presence of noise. Therefore, due to its superior performance as stated above, in the present paper, the basic ICA is used as an optimizer in solving damage detection problems.

In practical damage detection problems, as the available sensors are limited compared with the number of degrees of freedom, a large number of measurements at many locations may be required to accurately characterise the mode shape vector [24, 25]. The measurements, however, can be decreased by using the stiffness distribution over the structure, determined by damage functions [24-26]. Damage function effectively reduces the design variables and ensures a physically significant solution. Teughels et al. [24] used a finite element model updating method and damage function approach for damage assessment. The procedure was verified by a modal test of reinforced concrete beam. The algorithm produced a damage pattern which corresponded well with that obtained from the direct stiffness method. However, the damage location and severity were determined approximately. Zhang et al. [26] used the finite element model updating method and wavelet as damage functions to detect local damage. The numerical and experimental verifications showed better accuracy as well as higher computational efficiency [26]. They concluded that wavelet is more suited for local damage detection; therefore, it can only serve as a supplement to the traditional damage functions, rather than replacing them. Feature selection methods are another group of methods which may be used for decreasing design parameters [27, 28]. However, it appears that these are computationally more expensive than many heuristic methods to reach a relevant solution [29].

In using modal data, the majority of the available damage detection solution techniques discussed above, either require data for all the modes, or all the nodal data for a number of modes [9, 11, 20, 22], neither of which may be practically available through experiments. In the present study, damage identification problem is solved in a practical manner using a limited number of nodal data of a limited number of modes. The proposed method uses the imperialist competitive algorithm and damage functions. To decrease the number of design variables, several bilinear damage functions are defined to model the damage distribution. In previous studies, damage functions were defined as functions with constant widths and variable weights [24, 25]. However, using damage functions, the predicted damage location does not usually fit to the exact damage location [26, 30]. In the present study, to increase the accuracy of detecting damage location, the widths of the damage functions are also proposed to be variable in addition to the weights. Four different types of objective functions which use modal responses of damaged structure are investigated with the aim of finding the most suitable function. The efficiency and accuracy of the proposed method are investigated using three benchmark numerical examples using both clean and noisy modal data.

This paper is organized as follows: the backgrounds to the basic concepts used in this research, including: damage detection, damage functions and imperialist competitive algorithm, are discussed in Section 2. In Section 3, the proposed method is presented. Then, three benchmark case studies, a cantilever beam, a 40-element continuous beam and a plane portal frame, are solved and verified in Section 4. The parameters of the proposed method are discussed in Section 4.1. In Section 4.2, three case studies are solved using the proposed method without noisy data. The proposed algorithm is also verified using noisy data in Section 4.3. Finally, the conclusions end the paper in Section 5.

2. Background

2.1 Damage detection

Dynamic properties of a structure such as its natural frequencies and mode shapes are changed due to damage. These changes can be used to identify the damage properties, including its location and extent. Therefore, to solve the damage detection problem, a damage state has to be analytically found by which the analytical responses of the structure match the measured damage structure in an optimal manner. The problem can be defined mathematically as [11]:

$$\mathbf{R}_d = \mathbf{R}(\mathbf{X}) \Rightarrow \mathbf{X} = ? \qquad (1)$$

where, $\mathbf{R}_d$ and $\mathbf{R}$ are the response vectors of the measured and modelled structures, respectively. $\mathbf{X} = \{x_1, x_2, \ldots, x_n\}^T$ is the damage vector, in which x_i is the damage ratio of *i*th element, and *n* is the number of structural elements. As damage is considered to be modelled by a reduction in elastic modulus of the element, in this paper, x_i is defined as the ratio of the reduction in elastic modulus of damaged element to the elastic modulus of intact element. The ratio varies between 0 and 1, corresponding to the intact and completely damaged states. Based on Eq. (1), the problem can be expressed as minimizing the difference between the measured and modelled damage structural responses which can be solved by optimization methods. Therefore, the damage vector is the design variable of optimization process in solving damage detection problem. Since, in practice, the dimension of the damage vector is generally larger than the dimension of the measured response vector, the problem is mathematically undetermined. To overcome this problem, the dimension of damage vector can be decreased using the damage function method, as described in section 2.2.

2.2 Damage Functions

In damage detection problems, we generally have a set of experimental data (natural mode shapes, natural frequencies, etc…). The idea behind using optimization methods in detecting damage parameters (damage location and extent) is to minimize the differences between the experimental and analytical modal data. In this research, modal data is used as structural response to solve damage detection problem. Instead of updating the absolute value of design variable vector, $\mathbf{X}$, its relative variation to the intact value vector, $\mathbf{X}_0$ (i.e. undamaged case), is chosen as the dimensionless updating parameter, **a,** as follow:

$$\mathbf{a} = -\frac{\mathbf{X} - \mathbf{X}_0}{\mathbf{X}_0} \tag{2}$$

If the design variable has a linear relation with the element stiffness matrix, it can be calculated using the updating parameter as follow:

$$\mathbf{K}_e = \mathbf{K}_e^0 (1 - \mathbf{a}) \tag{3}$$

where, $\mathbf{K}_e$ and $\mathbf{K}_e^0$ are the updated and the initial element stiffness matrices, respectively. In the damage detection problem, every element stiffness matrix is a variable that should be updated in the optimization algorithm. Therefore, a large number of updating parameters is required to describe the damage parameters which is hardly possible by only a few available modal responses. Besides, in practice, the damage pattern may not exactly fit one element and may cover a number of neighbouring elements. To overcome these problems, a damage distribution for the structure can be determined as the sum of several damage patterns, named as damage functions, $\boldsymbol{N}_i$. Therefore, instead of detecting the damage ratio for each element, weight of the damage functions should be identified to solve the problem and detect the damage properties over the structure. As the number of functions are much less than the number of elements, the design variables are decreased. The approximate distribution of updating parameter **a** over the model is a linear combination of damage functions as follows:

$$\mathbf{X}(x) = \mathbf{X}_0\big(1 - \mathbf{a}(x)\big) = \mathbf{X}_0\big(1 - \textstyle\sum_{i=1}^{n} \rho_i \boldsymbol{N}_i\,(x)\big) \tag{4}$$

where, n is the total number of damage functions, $\boldsymbol{N}_i$ and ρ_i are the i^{th} damage function and its weight, respectively.

2.3 Imperialist Competitive Algorithm

The basic imperialist competitive algorithm (ICA) has been used previously to solve damage detection problems [22, 23]. To enhance the solution speed and algorithm efficiency in minimizing the differences between the calculated and the actual response data of the damaged structure, in the present research, the basic ICA is improved by adopting the damage function method and including a crossover operator.

The ICA algorithm generates a random number of countries as initial population. Some of the countries are selected to be the imperialists and the remaining countries are colonized by these imperialists, collectively form an empire. An individual country in an N_{var} dimensional optimization problem, characterized as follows [13]:

$$country = [p_1, p_2, \dots, p_{Nvar}] \tag{5}$$

The initial population of size $N_{country}$ is produced and N_{imp} countries with the least costs are assigned as the imperialists. The remaining countries are assigned as colonies which are divided between the imperialists based on the power of imperialists. The normalized cost of an imperialist is determined by:

$$C_j = f_{cost}^{(imp,j)} - max_i\left(f_{cost}^{(imp,i)}\right) \tag{6}$$

where, $f_{cost}^{(imp,j)}$ is the cost of the nth imperialist, $max_i\left(f_{cost}^{(imp,i)}\right)$ is the highest cost among imperialists and C_n is the normalized cost of imperialists. The normalized power of each imperialist is defined based on its normalized cost function; therefore, the number of initial colonies for each empire is denoted by:

$$NC_j = Round\left(\left|\frac{c_j}{\sum_{i=1}^{N_{imp}} c_j}\right| . N_{col}\right) \quad (7)$$

where, N_{imp} is the number of imperialists, N_{col} is the total number of initial colonies and NC_n is the number of occupied colonies by the Nth empire, randomly chosen and given to the nth empire.

The next step is assimilation in which the absorption policy commences among the imperialists to possess more colonies in a competitive manner. Based on the power of each imperialist, the colony moves toward the imperialist by x unit along different socio-political axes such as culture, language and religion. x is a random variable determined by:

$$x \sim U(0, \beta \times d) \quad (8)$$

where, d is the initial distance between the colony and the imperialist, β is a random value between 1 and 2 with uniform distribution. Therefore, the new position of colonies could be calculated as:

$$\{x\}_{new} = \{x\}_{old} + U(0, \beta \times d) \times \{V_1\} \quad (9)$$

where, $\{V_1\}$ is the direction of movement from the old location of colony to the imperialist position. The total power of an imperialist is obtained by:

$$TC_n = f_{cost}^{(impn)} + \xi . \frac{\sum_{i=1}^{NC_n} f_{cost}^{(col,n)}}{NC_n} \quad (10)$$

where, TC_n is the total cost of nth empire, NC_n is the number of colonies belonging to the nth empire and ξ is a positive value ranging between 0 and 1. The cost of empire is highly affected by the colonies role as the value of ξ increases. ξ = 0.1 has given good results in most of implementations. The normalized total cost of n^{th} empire, NTC_n, is simply obtained by:

$$NTC_n = TC_n - \max_i\{TC_i\} \quad (11)$$

The possession probability of each empire is given by:

$$p_{p_n} = \left|\frac{NTC_n}{\sum_{i=1}^{N_{imp}} NTC_i}\right| \tag{12}$$

To divide the colonies among empires, vector P is formed as follows:

$$P = [p_{p_1}, p_{p_2}, \dots, p_{p_n}]. \tag{13}$$

Next, vector D is formed by subtracting R from P as:

$$D = P - R \tag{14}$$

where, R is a uniformly distributed random number created with the same size as P. Referring to vector D, the colony is handed to an empire whose relevant index in D is maximized. Finally, the powerless empires are eliminated and the algorithm stops if there is only one empire left, and if not, solution goes back to assimilation.

3. Proposed algorithm

As it was stated before, in previous studies, the damage functions were defined as functions with constant widths and variable weights [24, 25]. The resulted damage location using these damage functions does not generally fit to the exact damage location [26, 30]. To increase the accuracy of detecting damage location, the widths of the damage functions are also proposed to be variable in addition to the weights being variable. In this strategy, two groups of input parameters are defined: (i) the weight of damage function, ρ and (ii) the width of damage function, *w*. The weight of damage function is a continuous variable which varies between 0 and 1 and the width is a discrete variable based on the number of elements. The $\boldsymbol{N}_i$ selected damage functions and their proposed variables are schematically shown in Fig. 1, highlighting their variable weights and widths.

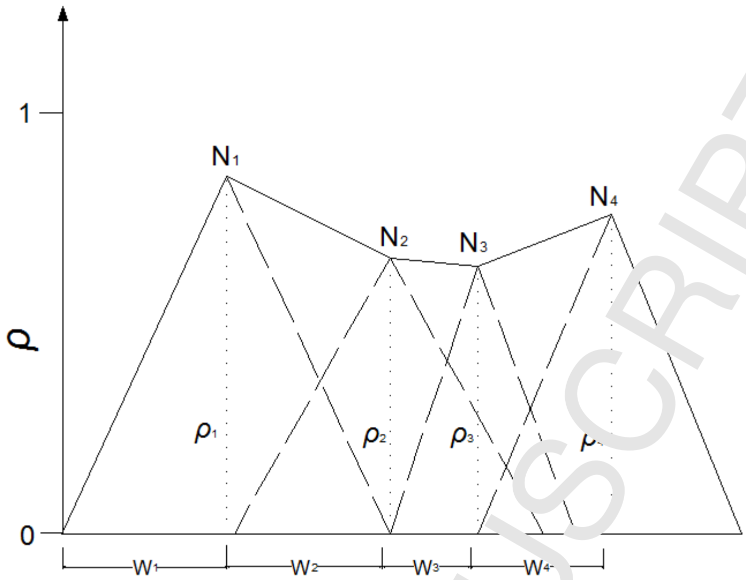

Fig. 1. Triangular-shaped damage functions (N_i) with varying weights (ρ_i) and widths (w_i)

As it was mentioned, the width of damage function is a discrete variable, whereas, the assimilation step of the ICA is set for continuous parameters. To overcome this problem, in this study, the crossover operator of the genetic algorithm (GA) is used instead for assimilation of width variables. In the GA crossover operation, two colonies are selected randomly and the crossover is carried out on *m* width variables as follows:

$$Colony_1 = \{x_1, \quad x_2, \quad x_3, \quad \cdots \quad x_{m-1}, \quad x_m\} \Rightarrow NewColony_1 = \{y_1, \quad y_2, \quad y_3, \quad \cdots, \quad y_{\alpha\times m}, \quad \cdots \quad x_{m-1}, \quad x_m\} \tag{15}$$

$$Colony_2 = \{y_1, \quad y_2, \quad y_3, \quad \cdots \quad y_{m-1}, \quad y_m\} \Rightarrow NewColony_2 = \{x_1, \quad x_2, \quad x_3, \quad \cdots, \quad x_{\alpha\times m}, \quad \cdots \quad y_{m-1}, \quad y_m\} \tag{16}$$

where, α is the percent of variables which would be exchanged in the two selected colonies for crossover operation. This value is set to 50% in this research based on [11]. The first α percent of m variables from the selected colonies would be exchanged.

Different objective functions may be specified in solving damage detection problems which use meta-heuristic optimization algorithms. Three different objective functions, termed OF_1, OF_2

and OF_3, have been used in the past with this class of problems using both natural frequencies and mode shapes. These objective functions are defined as follows:

1) The first objective function (OF_1) is defined as the norm of the difference vector of the analytical frequency responses, $\mathbf{R}_f(\mathbf{X})$, and the measured frequency responses of damaged structure, $\mathbf{R}_{df} = (r_{d1}, r_{d2}, \ldots, r_{dp})^T$, where p is the number of measured frequencies. i.e.:

$$\mathrm{OF}_1 = \left\| \mathbf{R}_f(\mathbf{X}) - \mathbf{R}_{df} \right\| \tag{17}$$

where, $\mathbf{X}=(x_1, x_2, \ldots, x_n)^T$ contains the design variables.

2) The value of multiple damage location assurance criterion (MDLAC) is considered as the second objective function, OF_2 [26].

3) The third objective function (OF_3) is to minimize the following cost value:

$$E_i = [\mathbf{K}^d - (\omega_i^m)^2 \mathbf{M}]\phi_i^m \quad i = 1, 2, \ldots, k \quad m = 1,2, \ldots, n \tag{18}$$

$$\mathrm{OF}_3 = \sqrt{\sum_{i=1}^{k} \left(\sum_{j=1}^{p} E_i^2 \right)} \tag{19}$$

in which, ω_i^m and ϕ_i^m are the i^{th} measured natural frequency and mode shape, respectively, k is the total number of mode shapes for damage detection and p is the number of DOF of the structure.

In the present study, a new, fourth objective function (OF_4), based on modal shape data is proposed. The proposed objective function is defined by the following equation:

$$\mathrm{OF}_4 = \left\| \frac{\mathbf{V}-\mathbf{V}_d}{\mathbf{V}_d} \right\| = \left\| \frac{\begin{Bmatrix} \mathbf{R}_1(\mathbf{X}) \\ w_{r1}\times\mathbf{R}_2(\mathbf{X}) \\ \vdots \\ w_{rm}\times\mathbf{R}_m(\mathbf{X}) \end{Bmatrix} - \begin{Bmatrix} \mathbf{R}_{d1}(\mathbf{X}) \\ w_{r1}\times\mathbf{R}_{d2}(\mathbf{X}) \\ \vdots \\ w_{rm}\times\mathbf{R}_{dm}(\mathbf{X}) \end{Bmatrix}}{\begin{Bmatrix} \mathbf{R}_{d1}(\mathbf{X}) \\ w_{r1}\times\mathbf{R}_{d2}(\mathbf{X}) \\ \vdots \\ w_{rm}\times\mathbf{R}_{dm}(\mathbf{X}) \end{Bmatrix}} \right\| \tag{20}$$

where, $\mathbf{R}_i(\mathbf{X})$ and $\mathbf{R}_{di}$ are the i^{th} vector of m mode shape responses of the modelled and measured damaged structures, respectively. Also, $\mathbf{X}=(x_1, x_2, \ldots, x_n)^T$ contains the design variables and w_{ri} is the i^{th} response weight value.

In damage detection problems, extent of damage is usually assumed to be uniform within the damaged element. Therefore, damage extent is conventionally expressed by only one variable corresponding to that element, x_i, whereas, the damage severities can be distributed non-uniformly within the damaged elements. To overcome this problem, the damage extent is described by nodal values. The stiffness matrices for the non-uniform elasticity distribution in damaged and intact cases are presented in ref. [9].

The pseudocode of the proposed method is as follows:

1- The initial countries are generated randomly with each country having two types of variables: damage function weight and width. The cost of each country is calculated and sorted in ascending order.
2- Based on the algorithm parameters and the main ICA, the initial empires are created.
3- The best imperialist position is defined.
4- The colonies of each empire are assimilated in this step. The weight variables of each colony are improved based on ICA assimilation, while the width variables are improved using the crossover operator of GA.
5- To converge the solution to a global minimum, the revolution stage of the ICA changes some colonies randomly. As the weight variables are continuous, they can be changed to random continuous values. Since, the width variables are discrete, they should be changed to random natural values.
6- The cost value of colonies in each empire are calculated and the total cost of each empire is evaluated.

7- The weakest colony from the weakest empire is selected and moved to the empire most likely to possess it.

8- The empire with no colonies is eliminated. Then, if the solution termination criterion is not satisfied, step 4 is repeated.

It should be noted that the above procedure is the same as that of basic ICA, except for the assimilation step of the algorithm (step 4). The flowchart of the proposed method is shown in Fig. 2.

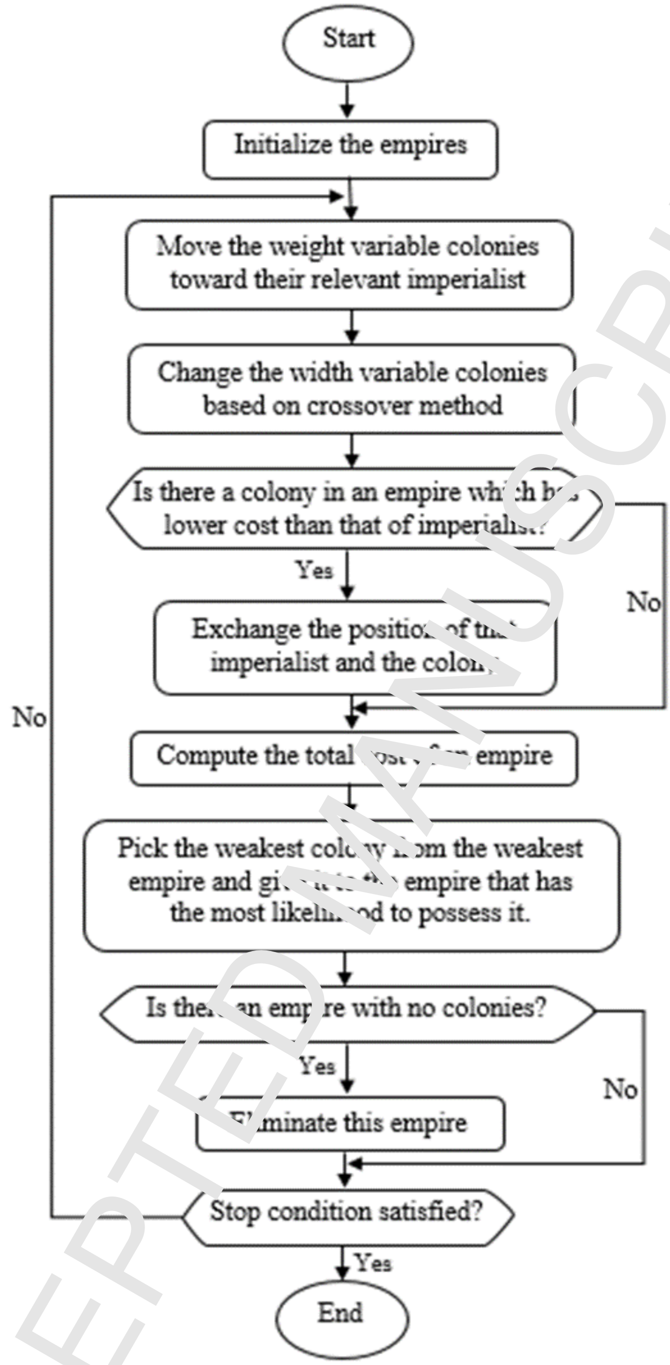

Fig. 2. Flowchart of the proposed method

4. Case studies

To assess the efficiency and accuracy of the proposed method, three benchmark problems have been chosen; a cantilever beam; a continuous beam and a plane portal frame. The problems are solved using the three existing and the new proposed objective functions specified earlier, so that appropriate comparisons can be made. To calculate the proposed objective function (OF_4), only the maximum nodal displacements of the first few modes are used. The objective function is multiplied by 500 so that the convergence of the algorithm is more clearly monitored. Damage is modelled by reducing the elastic modulus of the element. In each case, the algorithm parameters are set based on the size of the problem and previous recommendations as discussed below. Results of each case study are compared with those obtained from solution by other methods reported in the literature. The proposed algorithm is also verified using noisy data. The proposed method was implemented in and the structures were modelled by Matlab software on a system with 2 cores and 4 GB RAM properties.

4.1 Parameters of the proposed method

The parameters of the proposed method are selected for each case study as listed in Table 1. The number of colonies, iterations and shape functions depend on the size of the problem, i.e. the number of elements in the structure. Higher values of these parameters should be used as the number of elements increase. In the first case study (cantilever beam), the number of colonies and imperialists were selected as 100 and 10, respectively, based on recommendation made by previous researchers, solving similar problems with small number of elements (less than 30 elements) [20, 22]. However, as the other two case studies have more elements, the number of colonies was increased to 150. The maximum number of iterations for the first case study was set to 400, based on previous works solving problems with approximately similar number of elements [20, 22, 23]. As the other two case studies have more elements, the maximum iteration number for these cases were increased to 500 and 700, respectively. The selected iteration numbers are approximately equal or less than those in other works solving case studies with smaller number of elements [22, 23, 6]. The assimilation coefficient, β, is set equal to 2 in all cases based on recommendation in [18]. Also, the ICA revolution parameter (*rev*) is taken as 0.3 in all case studies based on the results of parametric investigation conducted by Maheri and Talezadeh [21]. The GA crossover percentage is selected as 80% based on recommendation given by Naseralavi et al. [11].

As the number of damage functions increase, the damage distribution will be more accurately evaluated, however, the cost of solution also increases. Therefore, an appropriate number of damage functions should be selected to solve the problem. In this research, the number of damage functions in each problem is determined by dividing the number of elements in that problem by 5 and rounding the result to an integer number. One damage function more or less than the resulted number may also be used based on the case study and user decision. The width of damage functions, *w*, is a discrete variable which varies based on the number of elements and damage functions, as given in the last column of Table 1.

Table 1. Parameters used in the solution of case studies

Case study	**parameter**							
	No. of colonies (*NC*)	No. of imperialists (*Imp*)	No. of iterations (*Itr*)	β	rev.	Crossover %	No. of shape functions	*w*
25-element cantilever beam	100	10	400	2	0.3	80	4	2, 3, 4, 5
40-element continuous beam	150	10	500	2	0.3	80	8	2, 3, 4, 5
56-element plan portal frame	150	10	700	2	0.3	80	12	2, 3, 4, 5, 6

4.2 Damage detection without noisy data

4.2.1 Cantilever beam

A cantilever beam, previously studied by Koh and Dyke [13] is considered as the first case study. The beam is modelled with 25 elements, as shown in Fig. 3, to increase the design variables. The length, thickness and width of the beam are 2.74m, 0.00635m and 0.0760m, respectively and the elements are numbered starting from the fixed end as shown in Fig. 3. The objective functions are determined using the displacements of 6 nodes in the first 3 mode shapes. The mode shapes were considered without noise.

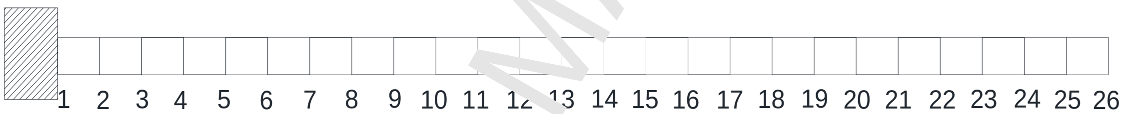

Fig. 3. Cantilever beam idealized with 25 elements

The elemental stiffness matrix of the beam for the non-uniform elasticity distribution is defined as:

$$\mathbf{K}_L^e = \frac{E_L I}{l^3}\begin{pmatrix} 6 & 4l & -6 & 2l \\ 4l & 3l^2 & -4l & l^2 \\ -6 & -4l & 6 & -2l \\ 2l & l^2 & -2l & l^2 \end{pmatrix} \tag{21}$$

$$\mathbf{K}_R^e = \frac{E_R I}{l^3}\begin{pmatrix} 6 & 2l & -6 & 4l \\ 2l & l^2 & -2l & l^2 \\ -6 & -2l & 6 & -4l \\ 4l & l^2 & -4l & 3l^2 \end{pmatrix} \tag{22}$$

$$\mathbf{K}^e = \mathbf{K}_R^e + \mathbf{K}_L^e \tag{23}$$

in which, $\mathbf{K}_L^e$, $\mathbf{K}_R^e$, E_L and E_R are stiffness matrices and elastic modulus of the left and right nodes of the element, respectively. The stiffness matrix of the beam element, $\mathbf{K}^e$, is evaluated by Eq.

23. The damage is simulated by a reduction in elastic modulus of the nodes and defined as damage ratio according to Eq. 2. Two damage scenarios are assumed to occur: (i) the node number 13 is 30% damaged, (ii) the node numbers 7 and 21 are 10% damaged.

As it was discussed earlier, four different objective functions may be used in the proposed algorithm. To investigate which objective function performs better in this example, results of damage detection for both damage scenarios using different objective functions are given in Table 2. Also given in this table are results of solution of the same problem using the CGA-SBI-MS method [10], BP-CGA method [31] and the BP-PSO-MS method [17], as well as the real damage parameters. Table 2 indicates that the CGA-SBI-MS method correctly detects location of damage in scenario 1, but could not identify the correct damage location in scenario 2. On the other hand, BP-PSO-MS and BP-CGA detect the correct damage parameters exactly. Regarding the proposed method, the algorithm using the first objective function (OF_1) detects no damage locations and when using the second objective function (OF_2) identifies two nodes as damage locations in scenario 1 and one node in scenario 2. Only one of the nodes in scenario 1, N_{14}, as the neighbouring node of the exact damaged location (N_{13}) is closely detected, while the damage extent is wrong. According to [10], solving a damage detection problem using ICA and the third objective function (OF_3) converges to the exact solution only when all the mode shape data are used. However, in practice, it is not possible to measure all the mode shapes and only data from a few mode shapes may be available. Therefore, the mode shapes data used in evaluating OF_4 are used here to evaluate OF_3. The 3rd node is identified as damaged node in both scenarios when the objective function, OF_3, is used, which is also erroneous. The algorithm using the proposed fourth objective function, OF_4, however, correctly detects the N_{13} node as peak point of the damage pattern with approximately correct damage extent. The different algorithm results show that only the fourth objective function, OF_4, has been able to correctly identify the damage locations and extents, compared with other functions. Also, considering that OF_1 and OF_2 use frequencies and OF_4 uses the mode shapes, it appears that the mode shape data is a more suitable structural response compared to natural frequency data in identifying the damage properties.

Table 2. Damage detection results of 25-element beam using different methods (N_i=extent (%))

Algorithm		Detected damage elements	
		Scenario 1	Scenario 2
Proposed method	OF_1	-	-
	OF_2	N_8=100 N_{14}=100	N_{23}=94
	OF_3	N_3=19	N_3=79
	OF_4	N_{13}=21	N_7=7.3 N_{21}=7.3
CGA-SBI-MS		N_{13}=19 N_{19}=16	N_7=6 N_9=5 N_{19}=8 N_{22}=7
BP-CGA		N_{13}=30	N_7=10 N_{21}=10
BP-PSO-MS		N_{13}=30	N_7=10 N_{21}=10
Real damage		N_{13}=30	N_7=10 N_{21}=10

The best and average results of ten runs in damage scenario 1 using OF_4 are shown in Fig. 4.a. As the best and average results are exactly the same, the proposed algorithm converges to the correct damage location in all the runs. The detected damage extent is 21% while the exact value is 30%, therefore the result is relatively close to the real value. Convergence histories of the mean and minimum imperialist costs are also compared in Fig. 4.b. The algorithm converges to the final result after about 130 iterations. Although the initial population is random, the average of 10 convergence histories is close to the best result of the algorithm. Fig. 4.c and Fig. 4.d show the standard deviation (SD) and coefficient of variation (CV) of thirty runs, respectively. The average and real damage distribution values for these runs are also shown in Fig. 4.c. In this example, since the results are similar in all runs, the SD and CV values are close to zero.

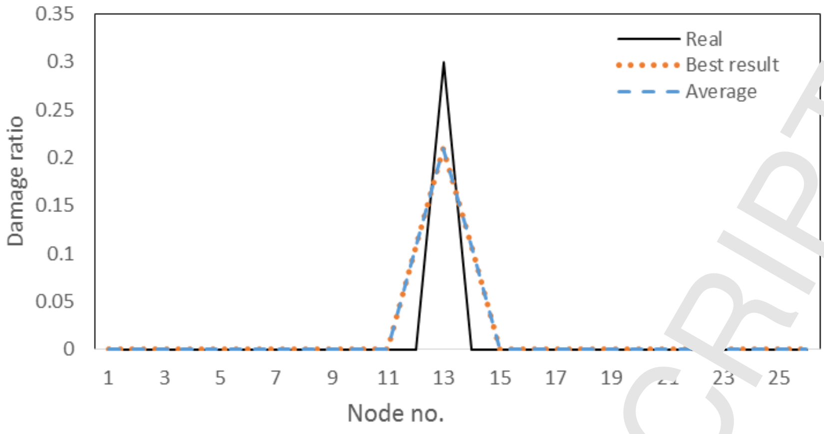
Real
Best result
Average
Damage ratio
Node no.

(a)

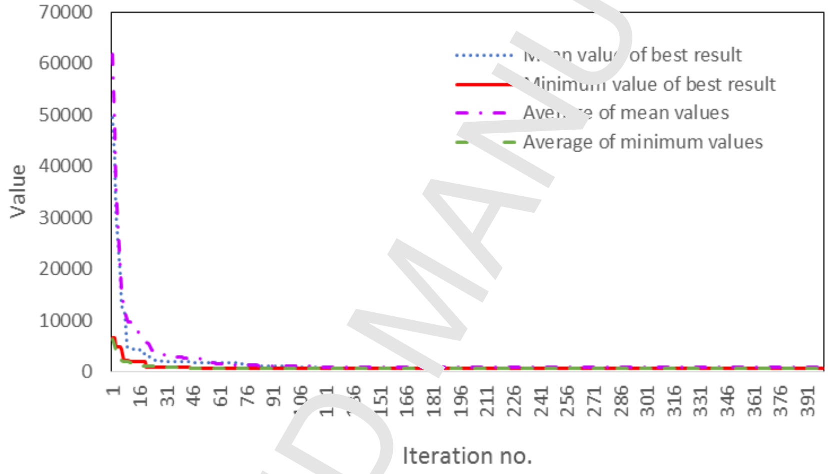
Value
Iteration no.
Average of minimum values

(b)

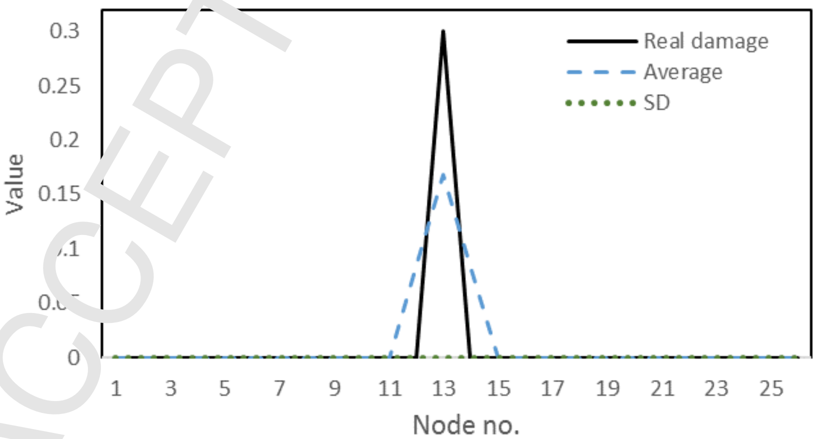
Real damage
Average
SD
Value
Node no.

(c)

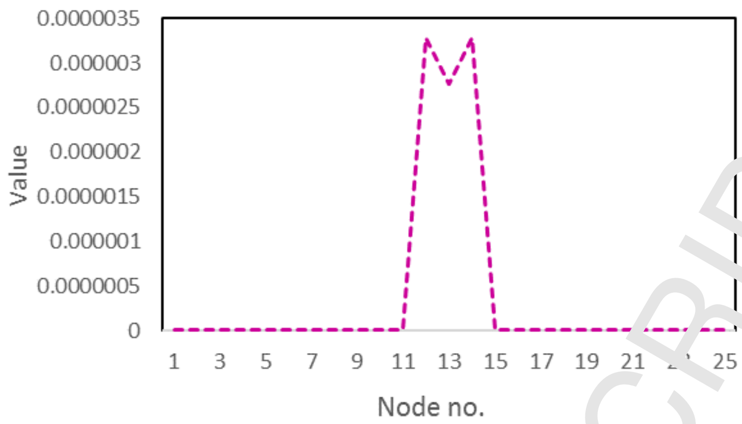

(d)

Fig. 4. Proposed algorithm results of cantilever beam damage scenario 1, using OF_4, (a) damage locations and extents, (b) convergence histories of mean and minimum imperialists cost values, (c) SD of thirty runs and (d) CV of thirty runs

The best and average results of ten runs in damage scenario 2 using the proposed OF_4 are shown in Fig. 5.a. It is evident that, the best result identifies the correct damaged nodes while the average result identifies the neighbouring nodes as the damaged nodes. As the elastic modulus of each node can affect the stiffness matrices of its two neighbouring elements, detecting a neighbour node as the damage location is logical. Using the proposed method gives the damage extents for scenario 2 damage as about 7.5%, which is relatively close to the exact value. Also, the better performance of the proposed OF_4 objective function compared to that of the OF_1 and OF_2, shows advantage of using mode shape data, compared to using frequency data.

Convergence histories of the mean and minimum imperialist costs are compared in Fig. 5.b. The algorithm converges after approximately 225 iterations and the convergence histories of the average and the best results are in close proximity. Based on the results of this case study, it can be stated that using damage functions with variable widths and OF_4 objective functions improved the performance of ICA to solve this damage detection problem with only a few mode shape data. Fig. 5.c and Fig. 5.d show the SD and CV values of thirty runs, respectively. The

ACCEPTED MANUSCRIPT

average and real damage distribution values are also shown in Fig. 5.c. It can be noted that the CV considerably decreases in damaged nodes.

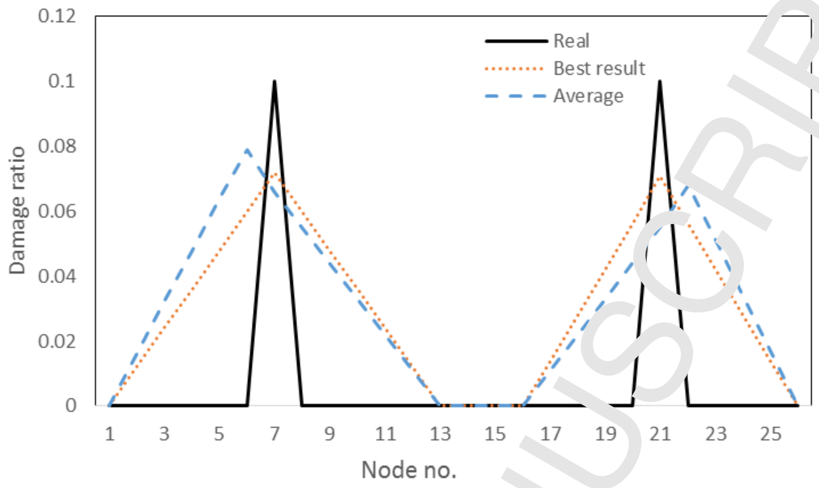

(a)

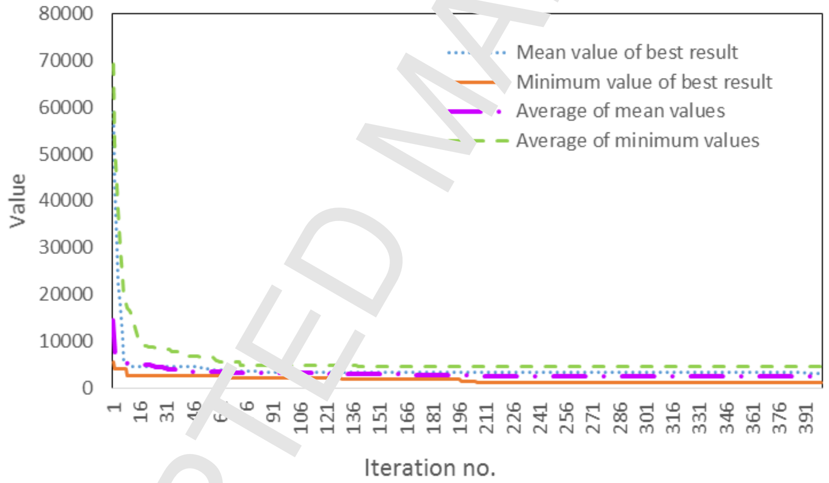

(b)

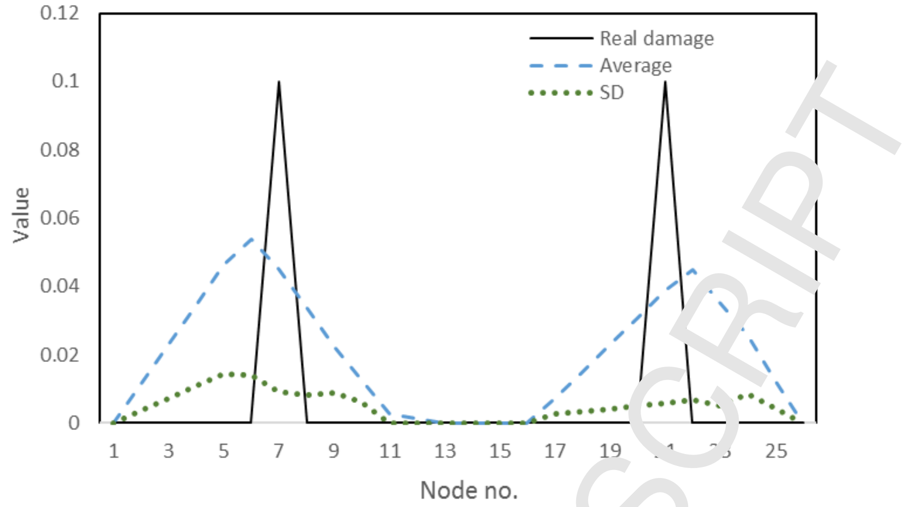

(c)

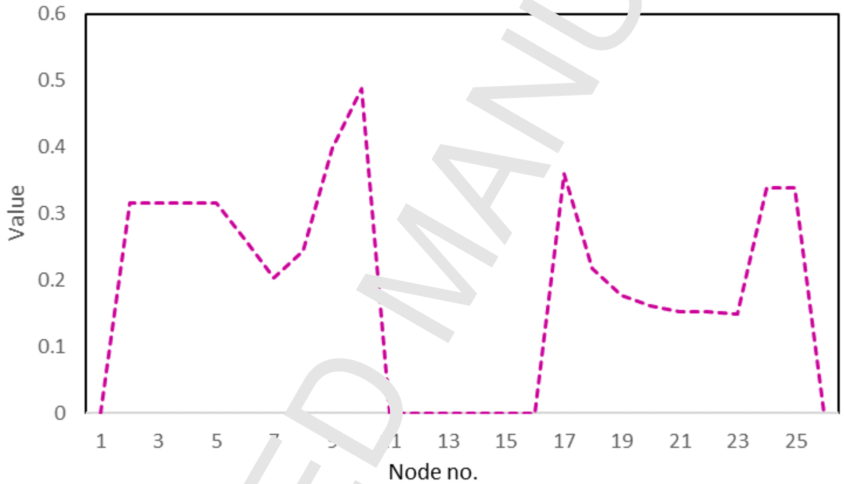

(d)

Fig. 5. Proposed algorithm results of cantilever beam, damage scenario 2, using OF_4, (a) damage locations and extents, (b) convergence histories of mean and minimum values, (c) SD of thirty runs and (d) CV of thirty runs

4.2.2 40-element continuous beam

The second numerical example is a 40-element continuous beam with two spans studied by Kaveh and Zolghadr [6] as shown in Fig. 6. The length, height, and width of the beam are 8m, 0.15m and 0.15m, respectively. The modulus of elasticity is 210 GPa and mass density is 7,860 kg/m^3. Each node has two degrees of freedom.

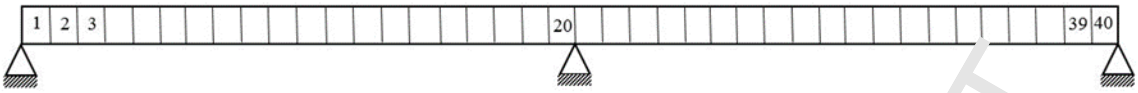

Fig. 6. 40-element continuous beam

Three different damage scenarios considered for the beam are shown in Table 3. The displacements of 8 nodes of the first 5 mode shapes are used in the proposed algorithm to solve the problem.

Table 3. Damage scenarios for the 40-element continuous beam (Damage extent =x%)

Scenario No.	Damaged element No. and extent
1	N_7=35 N_{20}=5 N_{37}=60
2	N_2=45 N_6=55 N_8=5 N_{26}=55 N_{32}=5
3	N_2=[illegible] $N_{[illegible]}$=50 N_{23}=5 N_{35}=50

The results of the proposed algorithm using different objective functions OF_1 to OF_4 are compared with the results from CGA-SBI-MS [8], BP-CGA [31] and BP-PSO-MS [17] methods in Table 4. Similar to the previous example, the algorithm using OF_1 detects no elements as damaged. Using OF_2 improves the results and one correct damaged node is detected in each scenario. The displacement mode shape data used in evaluating OF_4 are also used to evaluate OF_3. The algorithm with OF_3 also could not detect any damaged locations in scenario 1, but detects one damaged location in the other two scenarios. On the other hand, the algorithm with the proposed OF_4 converges to the correct damaged locations in all scenarios, except for the locations with small 5% damage extents in scenarios 2 and 3. Other damage extents are approximately predicted.

Regarding solutions by other methods, the CGA-SBI-MS and BP-CGA algorithm only detect one or two damaged locations in the first two scenarios and wrongly detect several elements in each scenario. The two algorithms are not able to identify the damage locations. The correct or a neighbouring node is detected in all scenarios by BP-PSO-MS, however, some other nodes are also incorrectly identified as damaged nodes. The estimated damage extents are also much higher than the exact values in most cases. This benchmark problem was also solved by Kaveh and Zolghadr [6], using the guided modal strain energy and tug-of-war optimization algorithm which utilised all nodal data from the first five mode shapes to reach exact damage locations and extents. Kaveh and Dadras [7] also solved scenarios 1 and 2 of this problem using the enhanced thermal exchange optimization algorithm which utilizes all the structural mode shapes. They reached exact solutions after 5000 iterations. Results from the two latter references are also given in Table 4.

Comparing the results of different algorithms, it is evident that the proposed method with the proposed objective function, OF_4, performs better than the CGA-SBI-MS, BP-CGA and BP-PSO-MS methods, however, it is less accurate than the solutions of references [6] and [7]. It should be noted that in these references all 40 nodal displacements of the modes are used to evaluate damage properties; something which is not very practical when using experimental data, whereas, in the proposed method, only 8 nodes of the first 5 mode shapes are used to solve the problem.

The best and average results of five runs using the proposed method with the proposed OF_4 objective function in damage scenario 1 are presented in Fig. 7. It can be seen that the algorithm is capable of detecting the exact damage locations not only in the best result but also on the average of results. The detected damage extent of the best and average results are also identified with good approximation. Fig. 7.c and Fig. 7.d show the SD and CV values of thirty runs, respectively. The average and real damage distribution values are also shown in Fig. 7.c. It can be seen that, the CV considerably decreases in the exact damaged nodes, while it increases in other nodes.

Table 4. Damage detection results of 40-element continuous beam using different methods

Algorithm		Detected damage elements		
		Scenario 1	Scenario 2	Scenario 3
Proposed method	OF_1	-	-	-
	OF_2	N_8=24 N_{25}=32 N_{32}=47	N_4=33 N_7=27 N_{30}=50	N_4=52 N_{11}=55 N_{36}=27
	OF_3	-	N_3=96 N_[illegible]=43	N_1=97
	OF_4	N_7=23 N_{20}=5 N_{37}=48	N_2=14 N_6=45 N_{26}=44	N_2=19 N_9=38 N_{36}=37
CGA-SBI-MS		N_2=25 N_4=12 N_{35}=30 N_{36}=25 N_{37}=47 N_{39}=23 N_{41}=80	N_1=23 N_2=42 N_6=37 N_7=47 N_{12}=16 N_{27}=54 N_{30}=28 N_{32}=43 N_{33}=25 N_{35}=16	N_2=15 N_{13}=78 N_{15}=62 N_{19}=76
BP-CGA		N_1=48 N_5=33 N_{23}=15 N_{24}=13 N_{36}=51	N_[illegible]=9 N_{15}=20 N_{16}=19 N_{27}=39 N_{34}=14 N_{35}=23 N_{36}=47	N_4=25 N_{18}=20 N_{23}=17 N_{33}=49 N_{37}= 11
BP-PSO-MS		N_5=19 N_6=29 N_{15}=20 N_{21}=29 N_{29}=10 N_{34}=33 N_{37}=73 N_{38}=45	N_1=54 N_5=84 N_{17}=85 N_{27}=35 N_{28}=44 N_{33}=8 N_{41}=38	N_3=71 N_6=42 N_{10}=95 N_{20}=47 N_{28}=87 N_{34}=95 N_{41}=95
Kaveh and Zolghadr [6]		E_7=35 E_{20}=5 E_{37}=60	E_2=45 E_6=55 E_8=4 E_{26}=55 E_{32}=6	E_2=35 E_9=50 E_{23}=5 E_{35}=50
Kaveh and Dadras [7]		E_7=36 E_{20}=6 E_{37}=60	E_2=44 E_6=55 E_8=6 E_{26}=55 E_{32}=6	-
Real damage		N_7=35 N_{20}=5 N_{37}=60	N_2=45 N_6=55 N_8=5 N_{26}=55 N_{32}=5	N_2=35 N_9=50 N_{23}=5 N_{35}=50

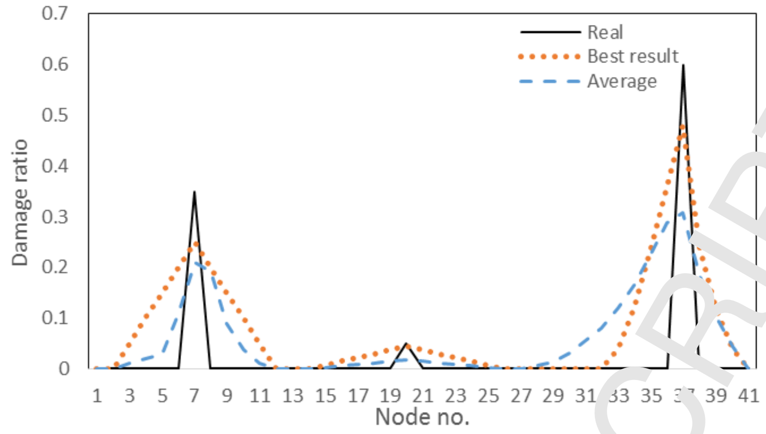

Real
Best result
Average
Damage ratio
Node no.

(a)

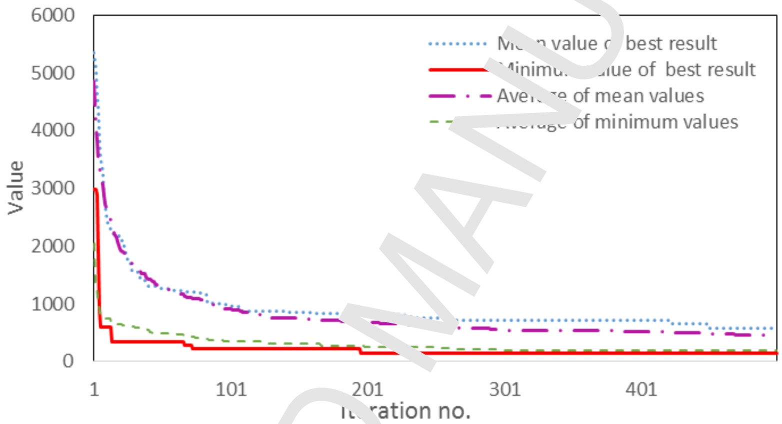

best result
value of best result
of mean values
of minimum values
Value

(b)

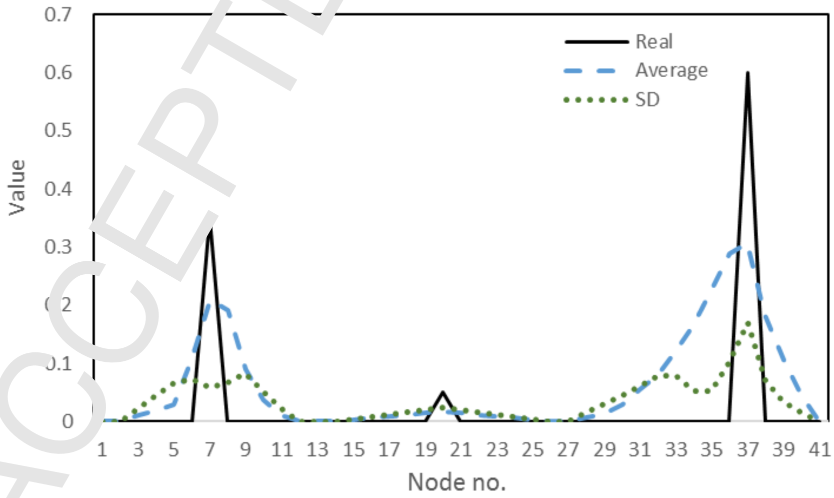

Real
Average
SD
Value
Node no.

(c)

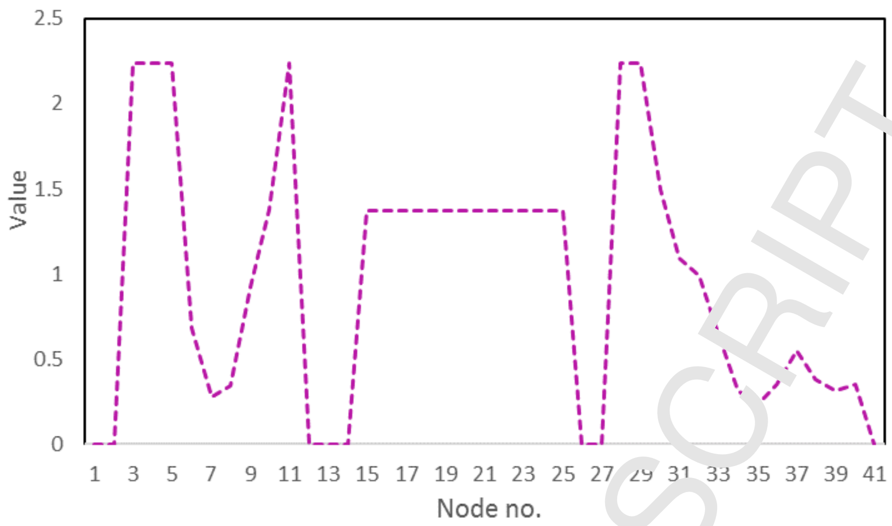

(d)

Fig. 7. Proposed algorithm results of 40-element continuous beam damage scenario 1, using OF_4, (a) damage locations and extents, (b) convergence history of mean and minimum values, (c) SD of thirty runs and (d) CV of thirty runs

The average and best results of damage scenario 2 using the proposed method with OF_4 objective function are shown in Fig. 8.a. The algorithm identifies the damage parameters of nodes 6 and 26 appropriately, however, the nodes number 8 and 32 are not clearly detected. These damage locations have very small extents (5%). As seen in Fig. 8.b, the histories of the best and average results converge approximately to the same result showing a smooth convergence of the proposed method. SD values of thirty runs are shown in Fig. 8.c, and their CV values are shown in Fig. 8.d. The average and real damage distribution values are also presented in Fig. 8.c. It can be noted that, similar to damage scenario 1, the CV effectively decreases in the exact damaged nodes while it increases in other nodes.

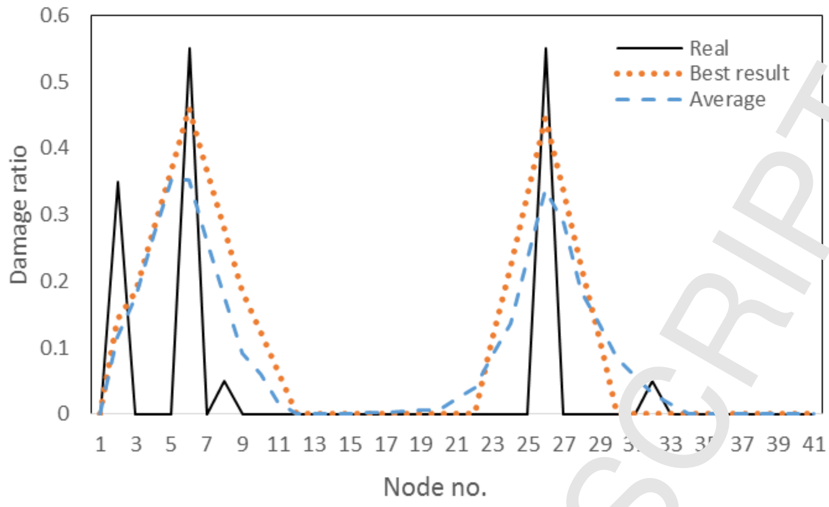

0.6
0.5
0.4
0.3
0.2
0.1
0
Damage ratio
Real
Best result
Average
1 3 5 7 9 11 13 15 17 19 21 23 25 27 29
37 39 41
Node no.

(a)

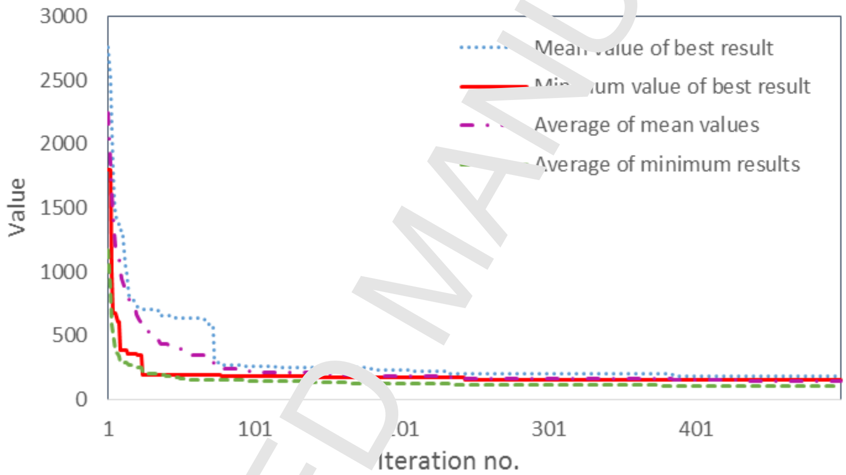

3000
2500
2000
1500
1000
500
0
Value
Average of mean values
1
101
301
401

(b)

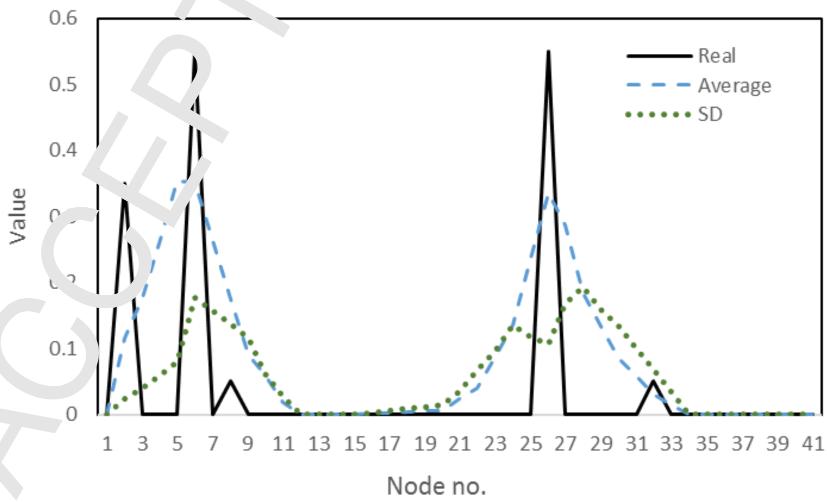

0.6
0.5
0.4
0.1
0
Value
Real
Average
SD
1 3 5 7 9 11 13 15 17 19 21 23 25 27 29 31 33 35 37 39 41
Node no.

(c)

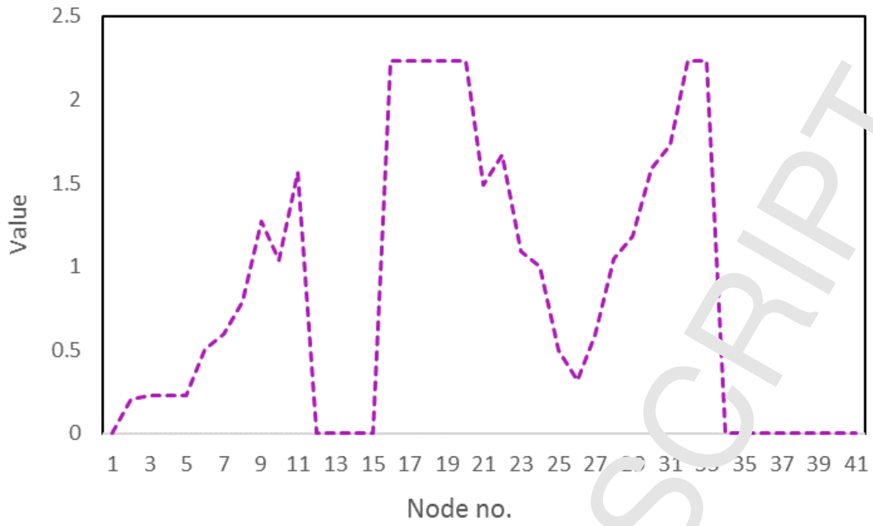

(d)

Fig. 8. Proposed algorithm results of 40-element continuous beam damage scenario 2, using OF_4, (a) damage locations and extents, (b) convergence history of mean and minimum values, (c) SD of thirty runs and (d) CV of thirty runs

Fig. 9 shows the results of damage scenario 3 using the proposed method. Based on the best result, the 9th and 2th nodes are detected correctly (Fig. 9.a). The 36th node is also identified as a damage location which is the neighbour of the actual damaged node number 35. The 23rd node, however, is not detected as it has a very low extent of 5%, although the shape function is deformed at this location. The average result is also approximately similar to the best result, indicating the robustness of the algorithm and the proposed objective function. The convergence histories of the best and average values, shown in Fig. 9.b, are also close to each other. The SD and CV values of thirty runs are respectively plotted in Fig. 8.c and Fig. 8.d. The average and real damage distribution values are also shown in Fig. 8.c. Similarly, the CV value noticeably decreases in the exact damaged nodes while it increases in other nodes.

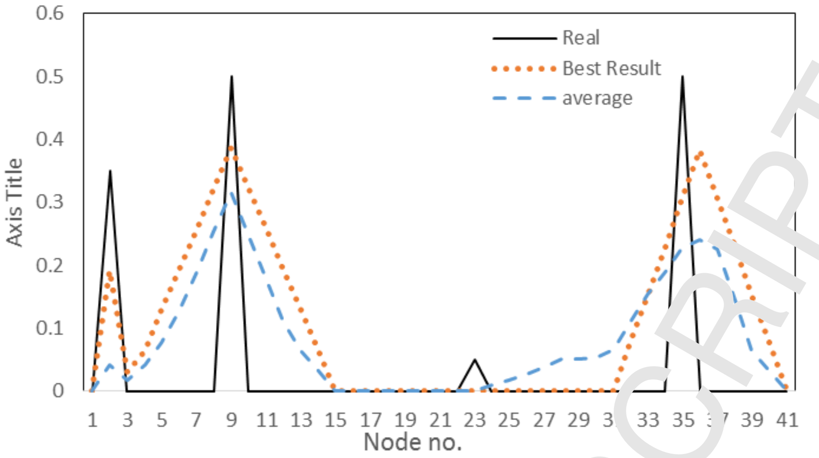
Real
Best Result
average
Axis Title
Node no.

(a)

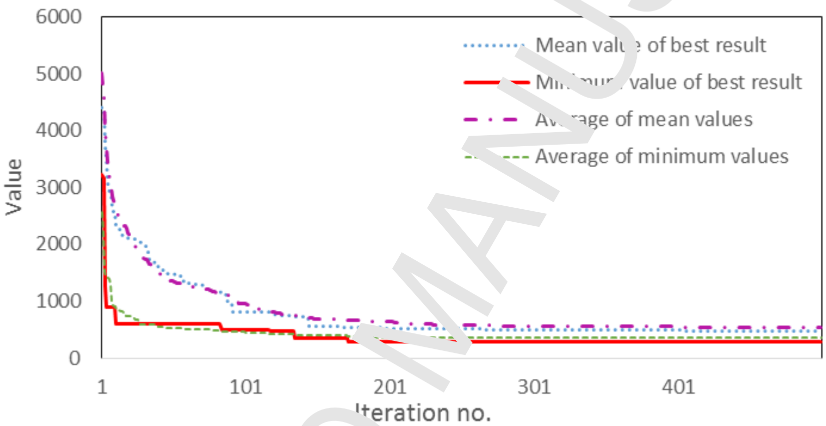
Mean value of best result
Minimum value of best result
Average of mean values
Average of minimum values
Value
Iteration no.

(b)

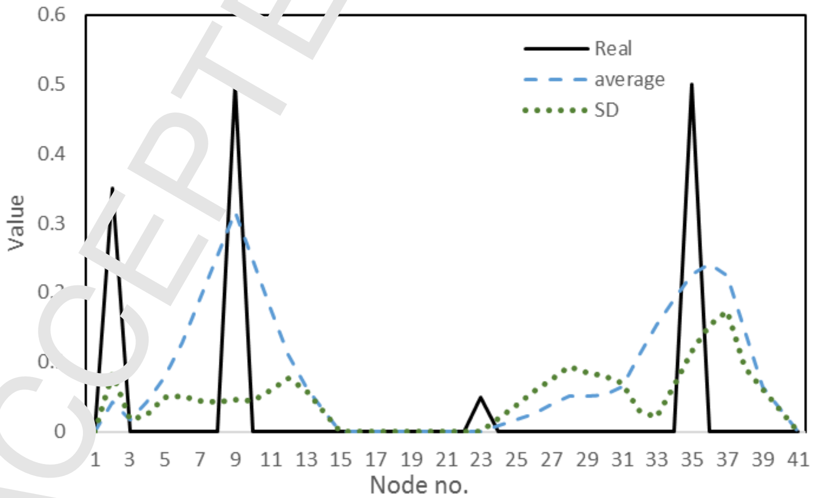
Real
average
SD
Value
Node no.

(c)

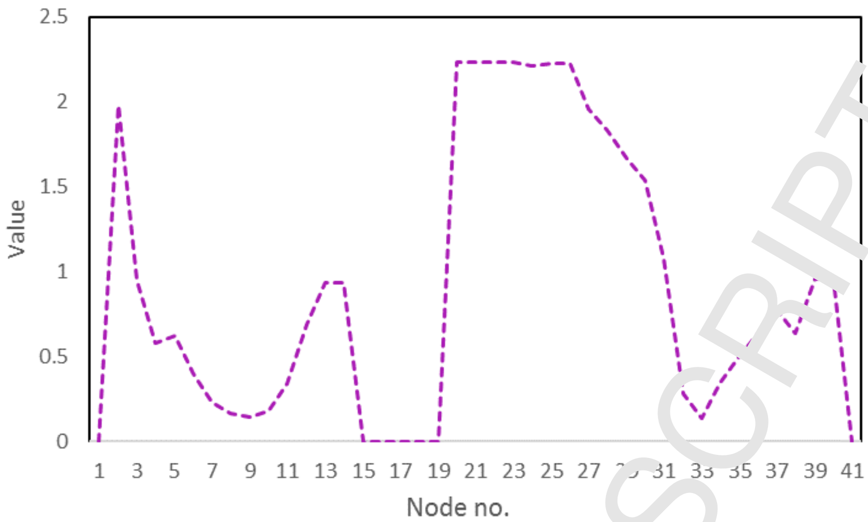

(d)

Fig. 9. Proposed algorithm results of 40-element continuous beam damage scenario 3 using OF_4, (a) damage locations and extents, (b) convergence history of mean and minimum values, (c) SD of thirty runs and (d) CV of thirty runs

4.2.3 Plane portal frame

To verify the ability of the proposed method in solving a larger problem with more variables, a portal frame investigated previously by V[illegible]zaga [32] is selected. The length and height of the portal frame are *L*=2.4 m and *H*=1.[illegible] m respectively. All frame elements have identical cross sectional dimensions of *h*=0.24 *m* and *b*=0.14 *m*. The material density is assumed to be 2.5×103 kg/m^3 and elastic modulus is taken as 2.5×1010 N/m^2. The finite element representation of this frame is shown in Fig. 10. Each node has two translational and one rotational degrees of freedom.

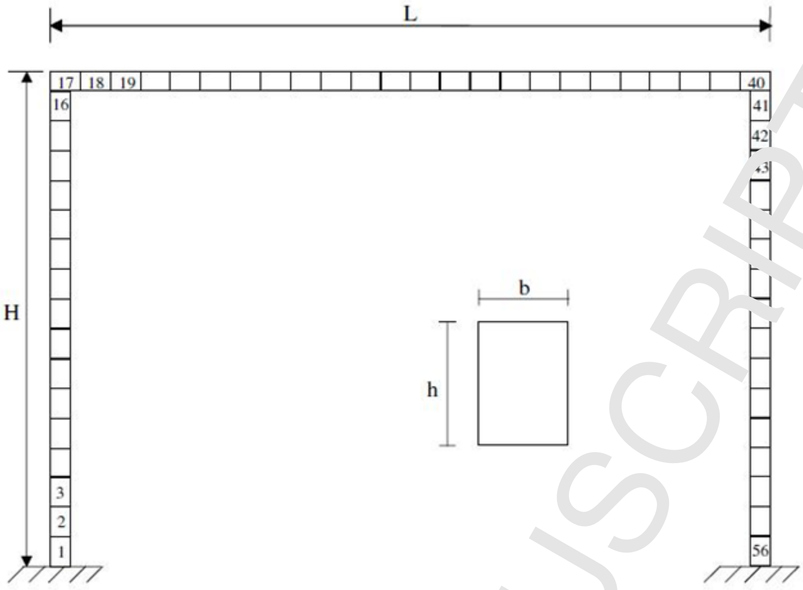

Fig. 10. The finite element representation of the plane portal frame

The elemental stiffness matrix of the frame for the non-uniform elasticity distribution is defined as:

$$\mathbf{K}_L^e = \frac{E_L I}{l^3}\begin{pmatrix} A\,l^2/2I & 0 & 0 & -A\,l^2/2I & 0 & 0 \\ 0 & 6 & 2l & 0 & -6 & 4l \\ 0 & 2l & l^2 & 0 & -2l & l^2 \\ -A\,l^2/2I & 0 & 0 & A\,l^2/2I & 0 & 0 \\ 0 & -6 & -2l & 0 & 6 & -4l \\ 0 & 4l & l^2 & 0 & -4l & 3l^2 \end{pmatrix} \tag{24}$$

$$\mathbf{K}_R^e = \frac{E_L I}{l^3}\begin{pmatrix} A\,l^2/2I & 0 & 0 & -A\,l^2/2I & 0 & 0 \\ 0 & 6 & 4l & 0 & -6 & 2l \\ 0 & 4l & 3l^2 & 0 & -4l & l^2 \\ -A\,l^2/2I & 0 & 0 & A\,l^2/2I & 0 & 0 \\ 0 & -6 & -4l & 0 & 6 & -2l \\ 0 & 2l & l^2 & 0 & -2l & l^2 \end{pmatrix} \tag{25}$$

$$\mathbf{K}^e = \mathbf{K}_R^e + \mathbf{K}_L^e \tag{26}$$

Three different damage scenarios are considered as described in Table 5. N_i is the i^{th} node of the frame. Ten nodal data of the first five modes are used as real damaged responses in calculating OF_3 and OF_4 and ten frequencies are used in establishing the other two objective functions (OF_1 and OF_2).

Table 5. Damage scenarios for the plane portal frame (Damage extent =x%).

Scenario No.	Damaged element No. and extent
1	N_7=10
2	N_{24}=30
3	N_{44}=10

Damage detection results of this frame using different methods are compared in Table 6. In damage scenario 1, the proposed algorithm using OF_1 detects the 51th node as the damaged node while the algorithm using OF_4 correctly detects the 7th node as the damaged location. As the frame is symmetric, changing the stiffness of the 51th and the 7th nodes has a similar effect on modal responses, however, the algorithm using OF_4 converges to the correct solution even in the symmetric case. The algorithm using OF_2 is unable to identify any damaged node and using OF_3 erroneously identifies a number of damaged locations. On the other hand, the proposed method with OF_4 objective function correctly identifies the exact damaged locations in all scenarios and the damage extents are also approximately identified.

This problem was also solved using other algorithms, including the CGA-SBI-MS method, BP-CGA method and the BP-PSO-MS method. As it is noted in Table 6, the CGA-SBI-MS solution was not able to detect the damage in any of the scenarios. The BP-CGA and BP-PSO-MS methods correctly identified the damage locations and extents in all scenarios.

This planar portal frame has also been solved by Gomes and Silva [33] using the Modal Sensitivity Analysis, as well as, GA and by Seyedpoor and Yazdanpanah [2] using MSEBI and SSEBI methods. In these studies, the damage parameters were set based on elements rather than nodes. Results from these four algorithms are also given in Table 6. In this table, E_i denotes the *i*th element. It can be seen that in Modal Sensitivity Analysis [33] for each damage scenario, the correct damaged element and another incorrect element are identified as damage locations. Also, in all scenarios the detected damage extents are considerably different compared to the actual extents. The results of GA [33] solution are approximately similar to those of the Modal Sensitivity Analysis [33]. The MSEBI [2] and SSEBI [2] solutions also converge to similar results in all scenarios. In scenarios 1 and 3, damage locations are identified correctly, however, damage extents are more than twice the actual values. Comparing the results from different solutions listed in Table 6, it can be stated that if non-noisy modal data is used, the proposed method with OF_2 and the BP-CGA and BP-PSO-MS methods are all powerful enough to correctly identify damage locations, however, the proposed method is less accurate than the other two methods in detecting damage extents.

To verify robustness of the algorithm with OF_4 objective function, the average result of ten runs is compared with the best result of damage scenario 1 in Fig. 11.a. The proposed method identifies the correct damaged node in the best result as well as in the average result. The best damage extent is approximately close to the exact value, the detected extent being 0.07 while the actual extent is 0.1. The best and average convergence histories of mean imperialists cost are very close to each other, so are the best and average minimum costs (Fig. 11.b). Therefore, the algorithm converges to similar results in almost all the runs. Fig. 11.c and Fig. 11.d show the SD and CV values of thirty runs, respectively. The average and real damage distribution values are also shown in Fig. 11.c. The CV is considerably less in the exact damaged nodes than in other nodes.

Table 6. Damage detection results of planar portal frame using different methods

Algorithm		Detected damaged elements		
		Scenario 1	Scenario 2	Scenario 3
Proposed method	OF_1	$N_{51}=5.2$	$N_{31}=16$	$N_{13}=5$
	OF_2	-	-	-
	OF_3	$N_4=100$ $N_{14}=140$ $N_{20}=83$ $N_{28}=140$ $N_{35}=103$ $N_{52}=140$	$N_4=120$ $N_{14}=105$ $N_{20}=100$ $N_{25}=100$ $N_{33}=100$ $N_{48}=120$	$N_{1[illegible]}=150$ $N_{20}=100$ $N_{[illegible]}=140$ $N_{35}=105$ $N_{47}=120$ $N_{55}=100$
	OF_4	$N_7=6.8$	$N_{24}=21$	$N_{44}=6.9$
CGA-SBI-MS		-	-	-
BP-CGA		$N_7=10$	$N_{24}=30$	$N_{44}=10$
BP-PSO-MS		$N_7=10$	$N_{24}=30$	$N_{44}=10$
Modal Sensitivity Analysis [33]		$E_7=6$ $E_{50}=6$	$E_{24}=1$[illegible] $E_{33}=1$[illegible]	$E_{13}=54$ $E_{44}=54$
GA [33]		$E_7=4$ $E_{50}=6.5$	$E_{24}=7.5$	$E_{13}=56$ $E_{44}=54$
MSEBI [2]		$E_7=22$	-	$E_{44}=23$
SSEBI [2]		$E_7=22$		$E_{44}=23$
Real damage		$N_7=10$	$N_{24}=30$	$N_{44}=10$

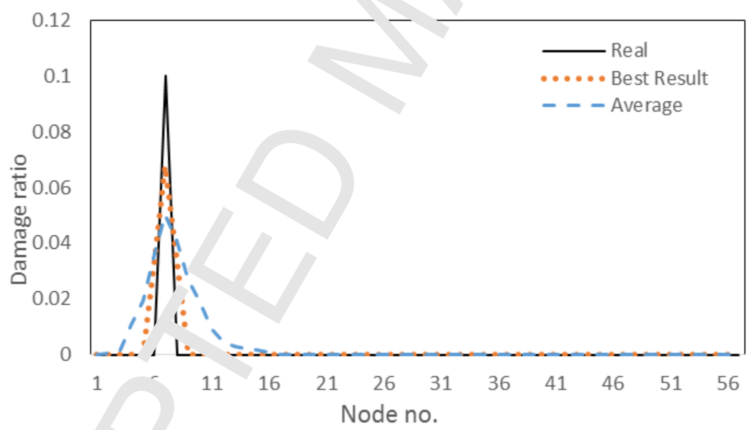

(a)

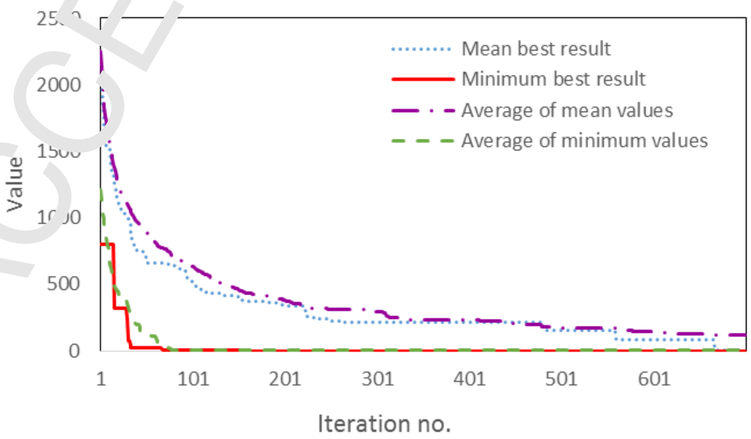

(b)

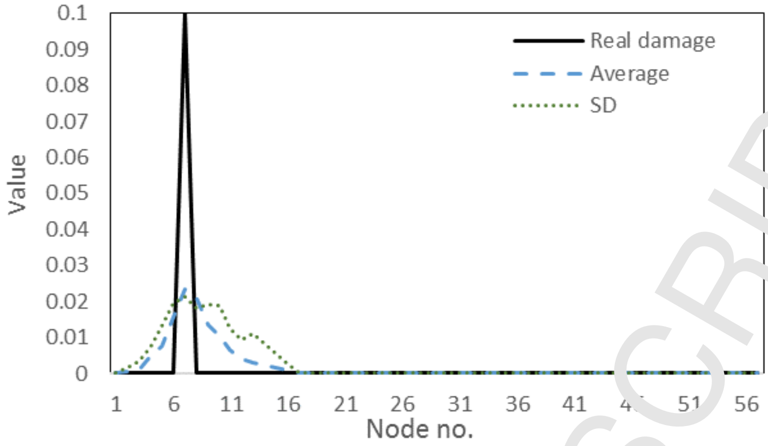

(c)

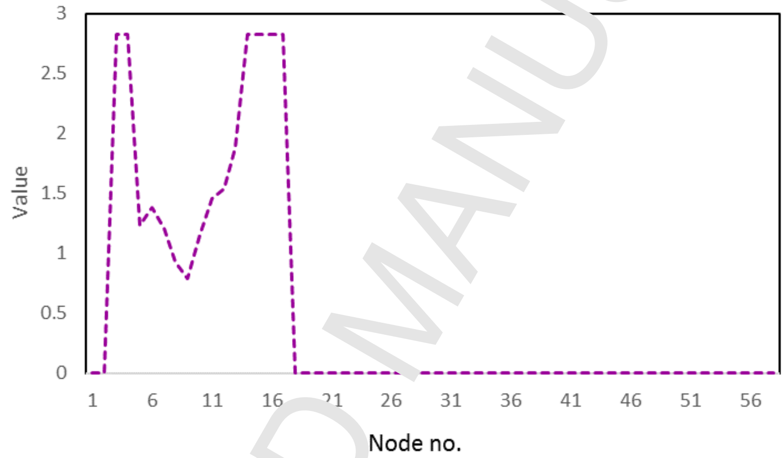

(d)

Fig. 11. Proposed algorithm results of plane frame, damage scenario 1, using OF_4, (a) damage locations and extents, (b) convergence histories of mean and minimum values, (c) SD of thirty runs and (d) CV of thirty runs

The average result of ten runs and the best result of the frame for damage scenario 2 evaluated using the proposed OF_4 are shown in Fig. 12.a. The best and average results of the algorithm detect the 24^{th} and 25^{th} nodes as damaged locations, respectively. Changing the left or right stiffness matrix of each element has an effect on the stiffness matrix of the two neighbouring elements. Therefore, it is logical to identify the neighbouring node as damaged node in some runs. The best identified damage extent in scenario 2 using the proposed method with OF_4 is 0.21 as compared to actual extent of 0.30. The best and average convergence histories of mean imperialists cost are also very close to each other, so are the best and average minimum costs (Fig. 12.b), which shows that the algorithm converges to similar results in almost all the runs. Fig. 12.c shows the SD, average and real damage distribution values, and Fig. 12.d shows the CV values for this problem, indicating that the CV value considerably decreases in the exact damaged nodes, while it increases in other nodes.

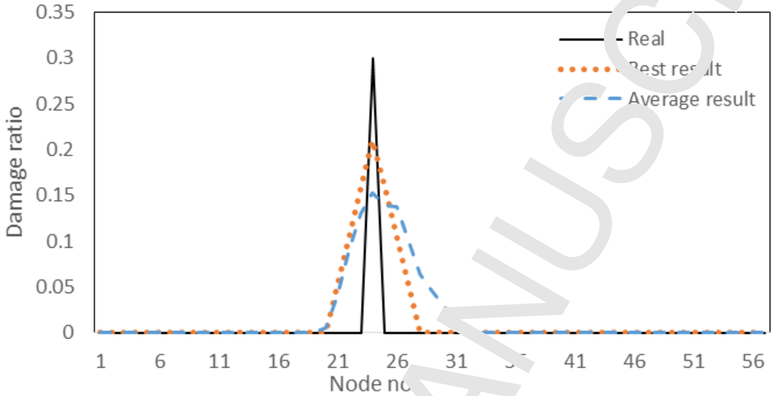

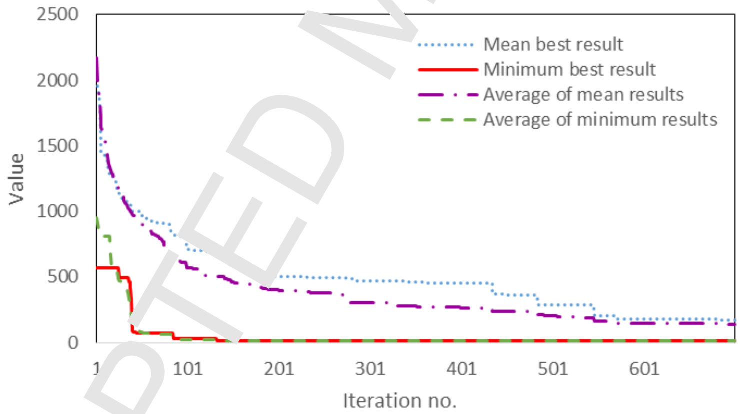

(b)

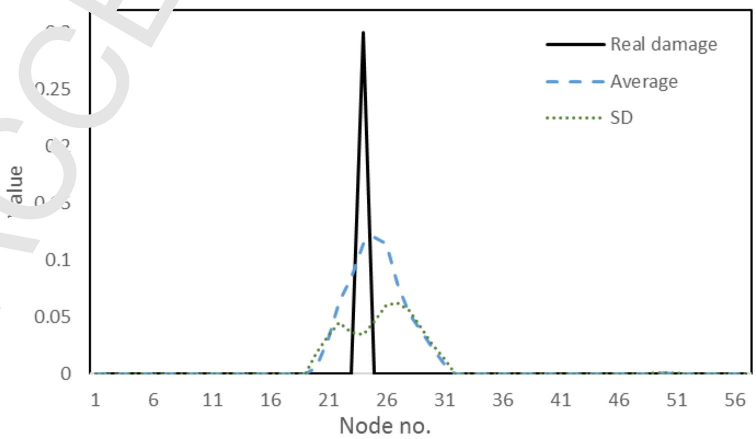

(c)

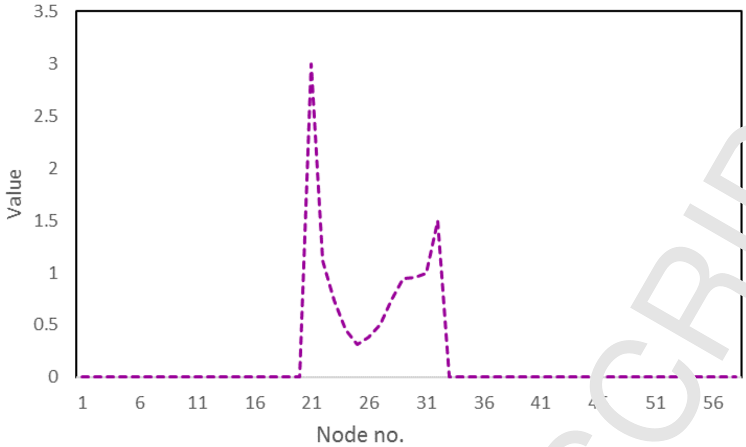

(d)

Fig. 12. Proposed algorithm results of plane portal frame, damage scenario 2, using OF_4, (a) damage locations and extents, (b) convergence histories of mean and minimum values, (c) SD of thirty runs and (d) CV of thirty runs

As shown in Fig. 13.a, the best and average results of the algorithm using OF4 detects the neighbouring, 45th node, as damaged location. The predicted damage extent is also 0.068 while the exact value is 0.1. In this scenario, the 27th node is also identified as a possible damage location in the average result. The best and average convergence histories of mean imperialists cost are shown in Fig. 13.b. The algorithm converges to the best result after 668 iterations. The closeness of the two sets of histories indicates that the algorithm converges to similar results in many of the runs. The SD, average and real damage distribution values of thirty runs for this problem are shown in Fig. 13.c and their CV is shown in Fig. 13.d.

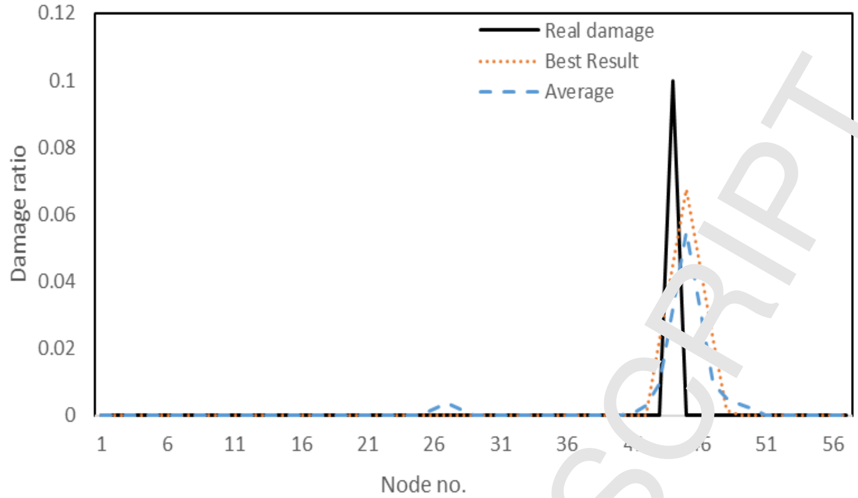
0.12
0.1
0.08
0.06
0.04
0.02
0
Damage ratio
Real damage
Best Result
Average
1
6
11
16
21
26
31
36
51
56
Node no.

(a)

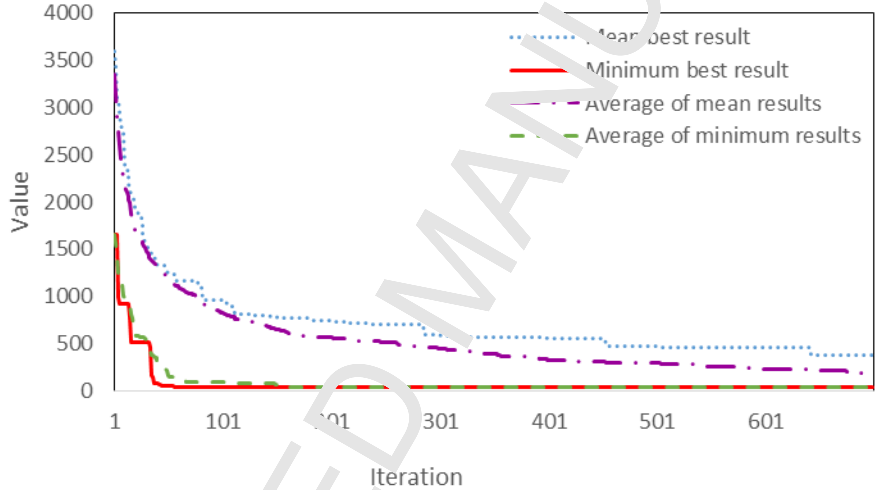
4000
3500
3000
2500
2000
1500
1000
500
0
Value
Minimum best result
Average of minimum results
1
101
301
401
501
601
Iteration

(b)

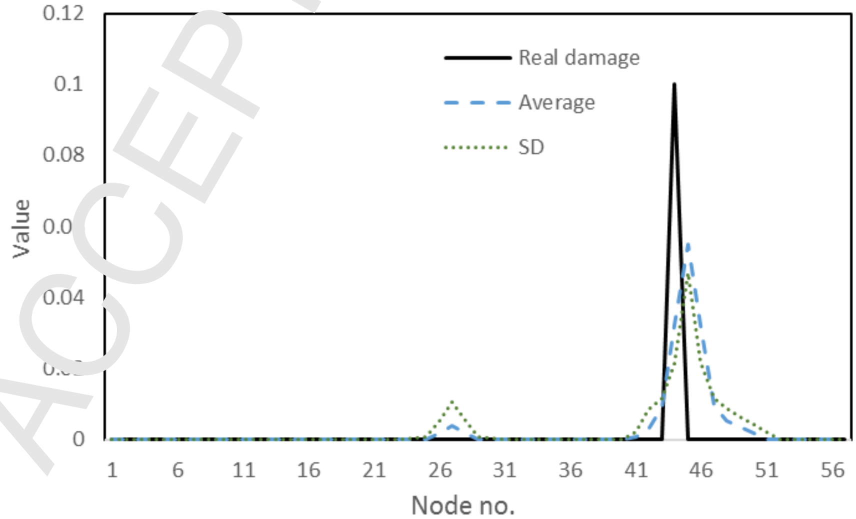
0.12
0.1
0.08
0.04
0
Value
Real damage
Average
SD
1
6
11
16
21
26
31
36
41
46
51
56
Node no.

(c)

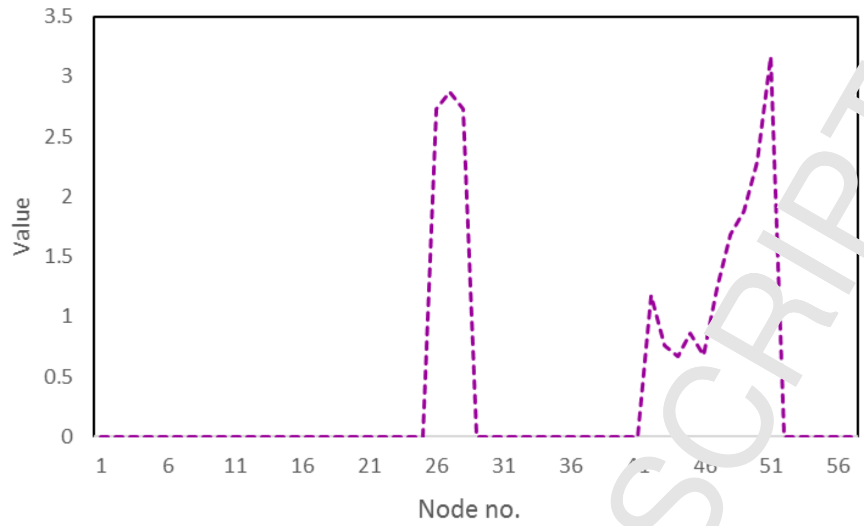

(d)

Fig. 13. Proposed algorithm results of plane portal frame, damage scenario 3, using OF_4, (a) damage location and extent, (b) convergence histories of mean and minimum values, (c) SD of thirty runs and (d) CV of thirty runs

4.3 Damage detection with noisy data

The experimental modal data are generally noisy. To further investigate the ability of the proposed method in solving practical damage detection problems, the noisy responses are used to identify the damage parameters. The noise is considered as a standard error for the modal responses. The solution results of the three benchmark problems using the proposed algorithm with non-noisy modal data, as discussed above, showed that the proposed objective function, OF_4, performs much better than the other three objective functions. Therefore, in damage detection investigation with noisy data, the proposed algorithm is used only with the proposed objective function, OF_4 and they are collectively termed: ‘the proposed method’.

4.3.1 Cantilever beam

To verify the ability of the proposed method of solving real problems with noisy data, 1% Gaussian white noise is added to the exact modal responses of the cantilever beam. All the other parameters were kept the same as those for the cantilever beam without noisy data, as discussed in section 4.2.1. The damage detection results using different methods with noisy data are shown in Table 7. The CGA-SBI-MS method could not detect the correct damage locations in any of the two damage scenarios. The BP-CGA method detects the correct damage location in scenario 1 but the extent is more than the actual value. In scenario 2, the damage locations are detected, however, two other locations are also wrongly detected as damaged. The detected damage extents of the 7th and 21th nodes are 7% and 11% which are not very far off the actual extents. The BP-PSO-MS method also detects the correct damaged locations in both scenarios but the damage extent in scenario 1 is 17% and in scenario 2, both detected damage extents are 45% which are very different to the actual values. The proposed method also correctly detects damage locations in both scenarios, furthermore, the evaluated damage extents in both scenarios are much closer to the real values.

Table 7. Damage detection results of 25-element beam using different methods using noisy data

Algorithm	Detected damaged elements	
	Scenario 1	Scenario 2
CGA-SBI-MS	N_{17}=14 N_{20}=22	N_{10}=5 N_{12}=9 N_{19}=7
BP-CGA	N_{13}=48	N_{7}=7 N_{8}=11 N_{20}=8 N_{21}=11
BP-PSO-MS	N_{13}=17	N_{7}=45 N_{21}=45
Proposed method	N_{13}=23	N_{7}=13 N_{21}=11
Real damage	N_{13}=30	N_{7}=10 N_{21}=10

The computational cost of the proposed method is compared with that of other solutions in Table 8. The proposed method converges to the correct damaged nodes after 200 iterations and 18100 analyses in 52 seconds. Although, in this example, the BP-PSO-MS, CGA-ABI-MS and BP-CGA methods converge faster than the proposed algorithm, the results obtained from the proposed method are more accurate.

Table 8. Computational cost of different methods for solving the 25-element beam

	Proposed method	CGA-SBI-MS	BP-PSO-MS	BP-CGA
Initial population	100	60	75	50
Iteration no.	200	40	60	40
Analysis no.	18100	8440	4758	3340
Time (Sec)	52	66	38	24

4.3.2 40-element continuous beam

For this problem, also 1.0 % Gaussian white noise is added to the exact modal responses. Other problem parameters are the same as those discussed in section 4.2.2. The damage detection results for this case study using different methods with noisy data are listed in Table 9. None of the CGA-SBI-MS, BP-CGA and BP-PSO-MS methods could detect the correct damage locations in scenario 1 and they only identified 1 or 2 of the damaged locations in the other two scenarios. Damage extents are also incorrectly estimated. In the guided modal strain energy and tug-of-war optimization method proposed by Kaveh and Zolghadr [6], all data of the first five mode shapes with 1% noise is used to solve this problem. The results, shown in Table 9, demonstrate that their algorithm has correctly identified the damaged locations with relatively accurate extents, however, in damage scenarios 2 and 3 some spurious nodes have also been identified as damaged. Kaveh and Dadras [7] applied the enhanced thermal exchange optimization algorithm to solve this damage detection problem in the first two scenarios, using all the mode shapes of the beam with 1% modal noise. The results of their study are also listed in Table 9. It is evident that their method accurately identifies damage locations and damage extents in both scenarios.

The proposed method also identifies the correct damaged nodes in all 3 scenarios, except for the nodes with the very small, 5% damage extent. The estimated damage extents are approximately similar to the results of the beam without noise and in some nodes the results even show improvements. This indicates that using noisy data does not affect the proposed method's convergence rate and accuracy. When comparing the results of the proposed method with those of references [6] and [7], it should be noted that the proposed algorithm solves the problem by using only 8 nodes data of the first five mode shapes, while data of all the nodes of the first five modes and the data of all the mode shapes of the beam are used in references [6] and [7], respectively. In practice, measuring all the mode shapes or all the nodal data of the first five modes is not normally possible, therefore, the proposed method offers a relatively accurate, practical alternative to those methods.

Table 9. Damage detection results of 40-element beam using different methods using noisy data

Algorithm	Detected damaged elements		
	Scenario 1	Scenario 2	Scenario 3
CGA-SBI-MS	N_2=25 N_3=15 N_5=29 N_6=13 N_{15}=42 $N_{[illegible]}$=27 N_{29}=27	N_1=22 N_2=16 N_4=31 N_5=20 N_6=70 N_7=27 N_{26}=33 N_{28}=21 N_{38}=33	N_1=11 N_{34}=17 N_{35}=55 N_{36}=17 N_{37}=15
BP-CGA	N_5=19 N_{16}=23 N_{17}=41 N_{21}=14 N_{27}=10 $N_{[illegible]}$=47	N_6=15 N_{15}=62 N_{21}=11 N_{26}=30 N_{33}=14 N_{35}=17	N_{17}=42 N_{20}=8 N_{34}=50 N_{35}=37
BP-PSO-MS	N_2=87 $N_{[illegible]}$=20 N_{26}=22 N_{36}=84 $N_{[illegible]}$=48	N_6=45 N_{13}=30 N_{27}=67 N_{30}=12 N_{36}=70 N_{41}=27	N_3=58 N_9=26 N_{10}=40 N_{17}=95 N_{18}=85 N_{30}=50
Kaveh and Zolghadr [6] (1% noise)	$E_{[illegible]}$=33 E_{20}=9 E_{37}=59	E_2=47 E_6=54 E_8=8 E_{15}=4 E_{26}=54 E_{32}=6 E_{37}=4	E_1=35 E_5=3 E_9=49 E_{23}=6 E_{35}=50
Kaveh and Dadras [7] (1% noise)	E_7=34 E_{20}=5 E_{37}=60	N_2=45 N_6=55 N_8=5 N_{26}=55 N_{32}=5	-
Proposed method	N_8=27 N_{37}=39	N_2=13 N_6=41 N_{26}=47	N_2=19 N_{10}=39 N_{34}=39
Real damage	N_7=35 N_{20}=5 N_{37}=60	N_2=45 N_6=55 N_8=5 N_{26}=55 N_{32}=5	N_2=35 N_9=50 N_{23}=5 N_{35}=50

Table 10 shows comparisons between the cost of the proposed method in solving this problem and costs of other solutions. The proposed method converges to the correct damaged nodes after 200 iterations and 26750 analyses in 179 seconds. The BP-PSO-MS and BP-CGA methods converge faster than the proposed algorithm, however, the results of the proposed method are more accurate compared with those solutions. On the other hand, the CGA-SBI-MS method is more costly compared with the proposed method and its results are less accurate.

Table 10. Computational cost of different methods for solving the 40-element beam

	Proposed method	CGA-SBI-MS	BP-PSO-MS	BP-CGA
Initial population	150	60	120	100
Iteration no.	190	4[illegible]	60	50
Analysis no.	26750	29500	12546	9150
Time (Sec)	179	706	139	118

4.3.3 Plane portal frame

In solving this problem with modal noise, 1.0% Gaussian white noise is also added to the modal data. Other problem parameters are the same as those discussed in section 4.2.3. Damage detection results of this frame using different methods with noisy data are shown in Table 11. The CGA-SBI-MS method is unable to solve the problem in any of the scenarios with the noisy data. The BP-CGA method only converges to the exact damage location and approximately half the damage extent in scenario 2. In each of the other two scenarios, one incorrect node is identified as damaged location. The BP-PSO-MS method respectively identifies the 7th and 44th nodes as damage location in scenarios 1 and 3, correctly. However, the method also detects 7 other nodes as damage location, incorrectly. The damage extents are also much more than the exact values. In scenario 2, 4 nodes are identified as damaged nodes, incorrectly.

Regarding the performance of the proposed method in the presence of noisy data, Table 11 shows that the exact damaged nodes in scenarios 2 and 3 are only correctly detected by the proposed method. Also, in scenario 1, the 8th node is identified as a damaged node which is the neighbour of the exact damaged node number 7. The damage extents are also approximately close to the exact values. Based on the results presented in Table 11, it is evident that the proposed method is able to solve the problem correctly in the presence of noisy data while other methods are not. Also, the detected damage extents are approximately similar to the results of Table 4 where the mode shapes were not noisy. Therefore, it appears that adding 1% noise to the modal responses not only does not affect the robustness and ability of the proposed method in solving the problem, it may actually enhance its performance. Tables 7, 9 and 11 indicate the abilities and advantages of the proposed method in solving larger damage detection problems compared with other methods.

Table 11. Damage detection results of planar portal frame using different methods and noisy data

Algorithm	Detected damage elements		
	Scenario 1	**Scenario 2**	**Scenario 3**
CGA-SBI-MS	-	-	-
BP-CGA	$N_{20}=31$	$N_{24}=17$	$N_{29}=18$
BP-PSO-MS	$N_7=84$ $N_8=95$ $N_9=95$ $N_{15}=95$ $N_{24}=57$ $N_{50}=95$ $N_{51}=95$ $N_{52}=72$	$N_9=25$ $N_{25}=87$ $N_{32}=95$ $N_{34}=95$	$N_{15}=95$ $N_{16}=21$ $N_{29}=84$ $N_{33}=95$ $N_{33}=95$ $N_{38}=79$ $N_{43}=95$ $N_{44}=67$
Proposed method	$N_8=7$	$N_{24}=23$	$N_{44}=6$
Real damage	$N_7=10$	$N_{24}=30$	$N_{44}=10$

The computational cost of the proposed method is compared with that of other solutions in Table 12. The proposed method converges to the correct damaged nodes after 160 iterations and 22550 analyses in 587 seconds. The BP-PSO-MS and BP-CGA methods converge faster than the proposed algorithm, however, the results of the proposed method are more accurate compared with those methods. On the other hand, the CGA-SBI-MS method is more costly compared with the proposed method, while producing less accurate results. In this and the previous problem, the difference in the number of analyses and running time of the proposed method and the BP-PSO-MS and BP-CGA methods decrease significantly compared with the smaller, 25-element beam problem. This indicates that, the efficiency of the proposed method increases for larger problems with increased number of nodes and design variables.

Table 12. Computational cost of different methods for solving planar portal frame

	Proposed method	CGA-SBI-MS	BP-PSO-MS	BP-CGA
Initial population	150	60	171	100
Iteration no.	160	4[illegible]	60	50
Analysis no.	22550	141600	20178	10700
Time (Sec)	587	5136	684	315

5. Conclusions

An algorithm was developed for detection of damage location and estimation of damage extent in structures on the basis of modal parameters of the damaged structure using imperialist competitive algorithm (ICA). In this method, damage functions have been used to model the damage pattern. To identify the correct damage location, the width of functions have been assumed to be variable. A new objective function (OF_4) is proposed and tested along with three other existing objective functions. Benchmark problems were solved with and without noise on the modal data. The following conclusions may be drawn from the results presented in this paper.

1- The proposed objective function (OF_4) which uses a limited number of mode shape data produces much better results compared to the previously proposed objective functions which use natural frequencies (OF_1 and OF_2). The proposed objective function (OF_4) is also more efficient than the cost value objective function using mode shapes and frequencies (OF_3).

2- The solutions of benchmark problems by the proposed algorithm, in most parts, converged to exact damage locations using only a few mode shapes data and the damage extents were also evaluated with acceptable approximation.

3- The proposed algorithm outperformed most other damage detection algorithms in detecting damage locations and extents. The algorithms which performed better than the proposed algorithm, generally require all the mode shape data which is not normally available.

4- The measured structural responses are generally noisy. The convergence of the proposed algorithm is stable in the presence of noisy data and in some cases, the algorithm performs even better with noisy modal data than with clean data, which makes it suitable as a practical damage detection technique.

5- Compared with other methods, the relative cost of solving damage detection problems using the proposed method decreases as the number of variables increases. Therefore, the proposed method is more cost-effective in solving larger problems, which makes it more useful in solving practical problems.

6- The proposed method is a practical, robust and efficient method to solve damage detection problems using only a few mode shape data, even if the data is noisy.

For further research, using other types of damage functions than those utilised here, such as higher order functions or wavelet functions, is proposed. Also, improving the revolution operator of the ICA and hybridizing ICA with other meta-heuristic algorithms may further improve the efficiency of the proposed method.

References

1- Q. Zhou, et al. The structural damage detection based on posteriori probability support vector machine and Dumpster–Shafer evidence theory. Applied Soft Computing, 2015;36:368-374.

2- Seyedpoor SM, Yazdanpanah O. An efficient indicator for structural damage localization using the change of strain energy based on static noisy data. Applied Mathematical Modelling, 2014;38:2661–2672.

3- D'Andreagiovanni F, Nardin A. Towards the fast and robust optimal design of wireless body area networks. Applied Soft Computing, 2015;37:971-982.

4- Blum C, Roli A, Aguilera M, Sampels M. Hybrid Metaheuristics - An Emerging Approach to Optimization. Springer, 2008, DOI: 10.1007/978-3-540-78295-7.

5- Chou JH, Ghaboussi J. Structural damage detection and identification using genetic algorithm. Proceedings of the international conference on artificial neural network in engineering, ANNIE'97, St. Louis, Missouri, 1997.

6- Kaveh A, Zolghadr A. Guided modal strain energy-based approach for structural damage identification using tug-of-war optimization algorithm, Journal of Computing in Civil Engineering, 2017;31(4). doi:10.1061/(ASCE)CP.1943-5487.0000665.

7- Kaveh A, Dadras A. Structural damage identification using an enhanced thermal exchange optimization algorithm. Engineering optimization, 2017; 1-22.

8- Kaveh A, Bakhshpoori T, Azimi M. Seismic optimal design of 3D steel frames using cuckoo search algorithm. Structural Design of Tall and Special Buildings, 2015;24(3):210-227.

9- Naseralavi SS, Gerist S, Salajegheh E, Salajegheh J, Elaborate structural damage detection using an improved genetic algorithm and modal data. International Journal of Structural Stability and Dynamics, 2013;13(6):57-76.

10- Vosoughi AR, Gerist S. New hybrid FE-PSO-CGAs sensitivity base technique for damage detection of laminated composite beams. Composite Structures, 2014;118:68-73.

11- Naseralavi SS, Salajegheh J, Salajegheh E, Fadaee MJ. An improved genetic algorithm using sensitivity analysis and micro search for damage detection, Asian Journal of Civil Engineering, 2010;11:717-740.

12- Mortazavi A, Toğan V. Sizing and layout design of truss structures under dynamic and static constraints with an integrated particle swarm optimization algorithm. Applied Soft Computing, 2017;5:239-252.

13- Koh BH, Dyke SJ. Structural health monitoring for flexible bridge structures using correlation and sensitivity of modal data. Computers and Structures, 2007;85:117-30.

14- Kang F, Li JJ, Xu Q. Damage detection based on improved particle swarm optimization using vibration data, Applied Soft Computing, 2012;12:2329-2335.

15- Chen Z, Yu L. A new structural damage detection strategy of hybrid PSO with Monte Carlo simulations and experimental verifications. Measurement, 2018;122:658-669.

16- Gambardella LM, Montemanni R, Weyland D. Coupling ant colony systems with strong local searches. European Journal of Operational Research, 2012; 220(3):831-843.

17- Gerist S, Maheri MR. Multi stage approach for structural damage detection problem using basis pursuit and particle swarm optimization, Journal of Sound and Vibration, 2016;384:210-226.

18- Atashpaz-Gargari E, Lucas C. Imperialist competitive algorithm: an algorithm for optimization inspired by imperialistic competition. In: IEEE congress on evolutionary computation, Singapore. 2007, 4661-7.

19- Rajabioun R, Atashpaz-Gargari E, Lucas C. Colonial competitive algorithm as a tool for Nash equilibrium point achievement. Lect. Notes. Computer and Science, 2008;5073:680-695

20- Nicknam A, Hosseini MH. Structural damage localization and evaluation based on modal data via a new evolutionary algorithm. Archive of Applied Mechanics, 2012;82:191-201.

21- Maheri MR, Talezadeh M. An Enhanced Imperialist Competitive Algorithm for optimum design of skeletal structures. Swarm and Evolutionary Computation, Online: Dec. 2017.

22- Bagheri H, Razeghi R, Ghodrati Amiri G. Detection and estimation of damage in structures using imperialist competitive algorithm. Shock and Vibration, 2012;19:405-419.

23- Zare Hosseinzadeh A, Bagheri A, Ghodrati Amiri G. Two-stage method for damage localization and quantification in high-rise shear frames based on the first mode shape slope. International Journal of Optimization in Civil Engineering, 2013;3(4):653-672.

24- Teughels A, Maeck J, De Roeck, G. Damage assessment by FE model updating using damage functions. Computers and Structures, 2002; 80:1869-1879.

25- Teughels A, De Roeck, G. Structural damage identification of the highway bridge Z24 by FE model updating. Journal of Sound and Vibration, 2004, 278:589–610.

26- Zhang W, Sun L, Zhang L. Local damage identification method using finite element model updating based on a new wavelet damage function. Advances in Structural Engineering, 2017:1–13. DOI: 10.1177/1369433217746837.

27- Mafarja, M, Mirjalili, S. Whale optimization approaches for wrapper feature selection, Applied Soft Computing, 2017;62:441-453.

28- Che J, Yang Y, Li L, Bai X, Zhang S, Deng C. Maximum relevance minimum common redundancy feature selection for nonlinear data. Information Sciences, 2017;68-86:409–410.

29- Mountassir ME, Yaccoubi S, Ragot J, Mourot G, Maquin D. Feature selection techniques for identifying the most relevant damage indices in SHM using guided Waves. 8th European Workshop On Structural Health Monitoring. 5-8 July, Spain, Bilbao, 2016.

30- Pereraa R, Ruiz A. A multistage FE updating procedure for damage identification in large-scale structures based on multi objective evolutionary optimization. Mechanical Systems and Signal Processing, 2008, 22:970–991.

31- Gerist S, Naseralavi SS, Salajegheh E. Basis pursuit based genetic algorithm for damage identification, International Journal of Optimization in Civil Engineering, 2012;2:301-319.

32- Veizaga JEF. Identificac¸ aode Danoem Estruturaspela Variac¸ aodas Caracterısticas Modais, Master Dissertation, PROMEC, Universidade Federaldo Rio Grandedo Sul, Portuguese, 1993.

33- Gomes HM, Silva NRS. Some comparisons for damage detection on structures using genetic algorithms and modal sensitivity method, Applied Mathematical Modelling, 2008;32:2216-2232.

List of Tables

List of Figures

- Imperialist competitive algorithm and damage functions are used to solve damage detection problem.
- Problem is solved using only a limited number of nodal data of a limited number of modes.
- Damage functions with variable widths are proposed for increased accuracy.
- A new objective function is proposed based on mode shape data.
- Three benchmark problems with both clean and noisy modal data are investigated.
- The new algorithm is most effective with real noisy modal data compared to other solutions.